Click Activated Protodrugs Against Cancer Increase the Therapeutic Potential of Chemotherapy through Local Capture and Activation

Kui Wu[1], Nathan A. Yee[2*], Sangeetha Srinivasan[2], Amir Mahmoodi[2], Michael Zakharian[2], Jose M. Mejia Oneto[2], Maksim Royzen[1]*

[*] Co-first authorship

[1] University at Albany, SUNY, 1400 Washington Ave., LS-1136, Albany, NY 12222
[2] Shasqi, Inc., 665 3rd St., Suite 501, San Francisco, CA 94107

Abstract

A desired goal of targeted cancer treatments is to achieve high tumor specificity with minimal side effects. Despite recent advances, this remains difficult to achieve in practice as most approaches rely on biomarkers or physiological differences between malignant and healthy tissue, and thus benefit only a subset of patients in need of treatment. To address this unmet need, we introduced a Click Activated Protodrugs Against Cancer (CAPAC) platform that enables targeted activation of drugs at a specific site in the body, i.e., a tumor. In contrast to antibodies (mAbs, ADCs) and other targeted approaches, the mechanism of action is based on *in vivo* click chemistry, and is thus independent of tumor biomarker expression or factors such as enzymatic activity, pH, or oxygen levels. The platform consists of a tetrazine-modified sodium hyaluronate-based biopolymer injected at a tumor site, followed by one or more doses of a *trans*-cyclooctene (TCO)-modified cytotoxic protodrug with attenuated activity administered systemically. The protodrug is captured locally by the biopolymer through an inverse electron-demand Diels-Alder reaction between tetrazine and TCO, followed by conversion to the active drug directly at the tumor site, thereby overcoming the systemic limitations of conventional chemotherapy or the need for specific biomarkers of traditional targeted therapy. Here, TCO-modified protodrugs of four prominent cytotoxics (doxorubicin, paclitaxel, etoposide and gemcitabine) are used, highlighting the modularity of the CAPAC platform. *In vitro* evaluation of cytotoxicity, solubility, stability and activation rendered the protodrug of doxorubicin, SQP33, as the most promising candidate for *in vivo* studies. Studies in rodents show that a single injection of the tetrazine-modified biopolymer, SQL70, efficiently captures SQP33 protodrug doses given at 10.8-times the maximum tolerated dose of conventional doxorubicin with greatly reduced systemic toxicity.

Introduction

Directing the activity of drugs to a location of the body where they are needed is a critical medicinal chemistry challenge, particularly with cytotoxic chemotherapy. Typically, only 1-2% of a systemically administered dose reaches the desired site i.e. the tumor, and as a result, these treatments are often associated with severe systemic adverse effects.[1] This limits the amount of drug that can be given to a patient safely. Thus, a critical challenge associated with cytotoxic chemotherapy drugs is their narrow therapeutic window. For example, doxorubicin (Dox) is a commonly used cytotoxic anthracycline drug with well-characterized and severe side effects. The antitumor activity of Dox is attributed to its interference of DNA replication by inhibiting topoisomerase II enzyme, and it has been used in the clinic to treat a variety of neoplastic conditions such as soft tissue sarcoma, acute lymphoblastic leukemia, acute myeloblastic leukemia, breast cancer, Kaposi's sarcoma and other types of cancer.[2] Despite its potent broad-spectrum antitumor activity, extended use of Dox in clinical practice is limited by life-threatening toxicities, with the most significant being largely irreversible and dose-dependent cardiotoxicity.[3] The short- and long-term toxic effects in the heart, ranging from alterations in myocardial structure and function, to congestive heart failure and severe cardiomyopathy. Congestive heart failure was reported in > 4%, > 18%, or 36% of patients who had received cumulative Dox doses of 500 to 550, 551 to 600, or > 601 mg/m^2, respectively.[4] In response, the clinical lifetime maximum dose of Dox is limited to 400–450 mg/m^2 in patients to minimize cardiotoxicity. However, this dose also limits the anti-tumor therapeutic benefit received by patients.[5] Treatment of solid tumors is an important example of an unmet medical need for novel strategies to efficiently focus cytotoxic activity locally, while sparing the rest of the body of deleterious toxic effects.

A number of drug delivery approaches have been developed in order to address these shortcomings. To improve the therapeutic window of Dox, targeted drug activation approaches have been developed in which Dox-based therapeutics with attenuated activity are administered systemically and activated in the body by inherent biological differences between cancerous and healthy tissue, such as pH[6], oxygen level[7], or protein expression.[8] Several such therapeutics have been developed by modifying the aminoglycoside portion of Dox with peptides, designed to be cleaved by proteases elevated in cancerous cells: *1*) L-377202 (Merck)[9-11], *2*) DTS-201 (or CPI-0004Na; Diatos)[8], and *3*) "Compound 5" (Bristol-Myers Squibb)[12]. The main benefit of cancer-activated therapeutics is that they may eliminate cancerous cells, while sparing healthy tissue from the cytotoxic effects. However, variability in the biological differences between cancerous and healthy tissue, as well as interpatient variabilities, are major limitations and current targeted activation approaches have failed to reach meaningful improvements to the safety profile of conventional Dox in the clinic.

In addition to dose-limiting toxicity, poor aqueous solubility is another obstacle in the systemic administration of well-established anticancer drugs, such as paclitaxel (PTX) and etoposide (ETP). Formulation of these drugs often requires organic co-solvents which restricts their utility in the clinic. PTX has been widely used to treat lung, breast, pancreatic and ovarian cancers.[13] This anti-microtubule diterpenoid triggers cellular apoptosis by blocking the progression of mitosis. Due to poor solubility, PTX is typically formulated using ethanol or polyethylated castor oil, Cremophor EL. This formulation can cause serious side-effects, such as peripheral neuropathy, hypotension, and hypersensitivity.[14-15] ETP is frequently used in combination with other chemotherapeutic agents to treat refractory testicular tumors, small-cell lung cancer, lymphoma, non-lymphocytic leukemia and glioblastoma multiforme.[16] ETP inhibits DNA topoisomerase II, thereby inhibiting DNA synthesis at the pre-mitotic stage. Due to poor aqueous solubility, administration of high-doses of ETP requires formulation in ethanol, polysorbate 80, benzyl alcohol, and polyethylene glycol and can cause hypotension and allergic reaction.[17-18]

In order to address these challenges, we developed the modular, Click Activated Protodrugs Against Cancer (CAPAC) platform, in which cytotoxics are activated locally through the combination of systemically administered protodrugs with attenuated toxicity, and a locally injected protodrug-activating biopolymer. Click chemistry-based approaches involve highly reactive and mutually selective chemical groups that minimally interact with natural mammalian physiology – thus the site-specific targeting is achieved through chemistry rather than relying on the inherent biological properties of the tumor.[19-22] The CAPAC platform is illustrated schematically in **Figure 1**, and involves 4 steps: (1) a biopolymer modified with tetrazine (Tz) groups is injected directly to a tumor site. (2) A protodrug form of a cytotoxic, which has been chemically attenuated by modification with *trans*-cyclooctene (TCO), is administered systemically. (3) The protodrug is captured at the biopolymer injection site (the targeted region) and removed from circulation through a covalent inverse electron-demand Diels Alder reaction between TCO and Tz, concentrating it to the desired site with precise spatial control. (4) A subsequent chemical reaction spontaneously releases the active drug. In this approach, the site-specific targeting is achieved through the chemical reactivity of Tz and TCO, rather than relying on the inherent biological properties of the tumor, resulting in a wider therapeutic window compared to other targeted approaches. Additionally, hydrophilic substituents can be incorporated to the TCO moiety, allowing for improved aqueous solubility of the protodrug over the parent compound.

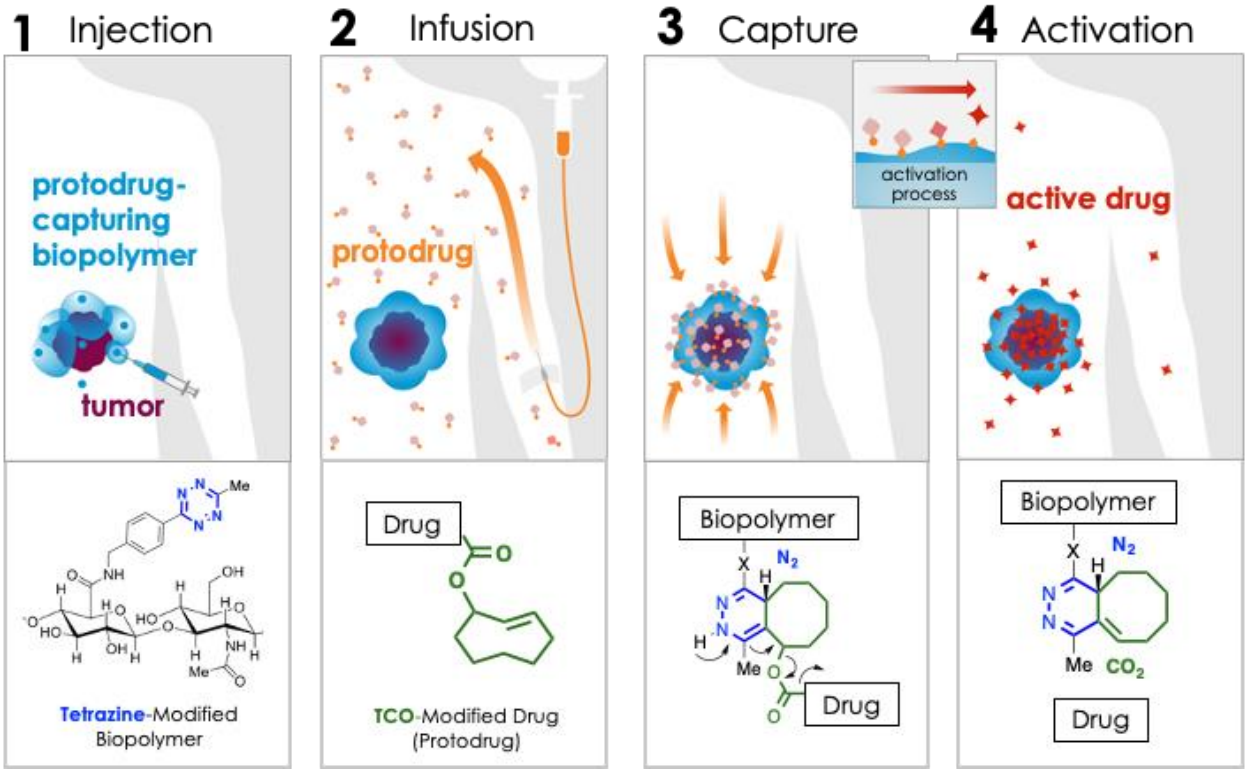

Figure 1. Mechanism of CAPAC platform: 1) Tetrazine-modified biopolymer is locally injected at the pathological site. 2) A TCO-modified drug (protodrug) is infused systemically. 3) The protodrug is captured by the biopolymer at the desired site through a rapid covalent reaction between Tz and TCO moieties, followed by 4) chemical rearrangement to release active drug.

Results and Discussion

We have previously demonstrated proof-of-concept and feasibility of the CAPAC platform in an animal model,[22] and showed enhanced safety and efficacy with a cytotoxic protodrug in a

mouse tumor model. [23] The CAPAC approach allowed a higher amount of a TCO-Dox protodrug to be given intravenously (IV) without adverse effects as compared with conventional Dox treatment, and furthermore, it showed complete response when treating a local fibrosarcoma in mice. However, clinical translation of the previous construct was problematic due to poor aqueous solubility of the TCO-Dox protodrug, which considerably limited the amount of treatment that could be given IV. Described herein, we incorporated hydrophilic groups to the TCO moiety in order to improve aqueous solubility of the resulting protodrugs. We also highlight the modularity of the CAPAC platform through synthesis of novel protodrugs of prominent small molecule chemotherapeutics like PTX, ETP and gemcitabine (GCB), in addition to Dox. We then evaluated the cytotoxicity, solubility, stability and activation of these protodrugs *in vitro* and identified the Dox protodrug, **SQP33**, as the best candidate for *in vivo* studies. SQP33 protodrug was tested *in vivo* with **SQL70** biopolymer, which is composed of sodium hyaluronate (NaHA), a non-sulfated glycosaminoglycan, modified with Tz. IV administration of SQP33 following a subcutaneous (SC) injection of SQL70 (together called **SQ3370** treatment) proved to be significantly less toxic than Dox hydrochloride (HCl), allowing markedly higher doses to be well-tolerated in *Sprague-Dawley* (SD) rats, with significantly reduced adverse cytotoxic exposure. Specifically, a cumulative SQP33 dose equivalent to 10.8-times the cumulative maximum tolerated dose (MTD) of Dox HCl was safely administered to these animals with significantly lower resultant Dox exposure observed in heart tissue (as compared to rats treated with Dox HCl). Furthermore, pharmacokinetic (PK) analysis confirmed the hypothesis that SQL70 biopolymer effectively captures SQP33 protodrug, resulting in release of active Dox at the desired site.

Protodrug Design, Synthesis and *In Vitro* Evaluation

Recognizing that the TCO moiety is only present at the protodrug stage led to the design of a second generation of protodrugs with improved aqueous solubility. Structural elements of TCO were explored to introduce additional hydrophilic groups, as illustrated in **Scheme 1**. At the core of the protodrug structures is a heterobifunctional TCO[24-25] bearing a carboxylic acid at a tertiary carbon, which was regioselectively modified with cytotoxic compounds on one end and functionalized with hydrophilic groups, such as glycine or aspartic acid on the other. Importantly, the TCO carboxylate used is 99% enantiomeric excess (*ee*) at that tertiary chiral carbon, so that only single diastereomers of the protodrugs are formed. Three general synthetic procedures have been developed that allow modular assembly of these constructs, while taking into account inherent sensitivity of Dox, PTX, ETP and GCB to various late stage chemistries. In principle, other amino acids or hydrophilic groups could be installed as desired.

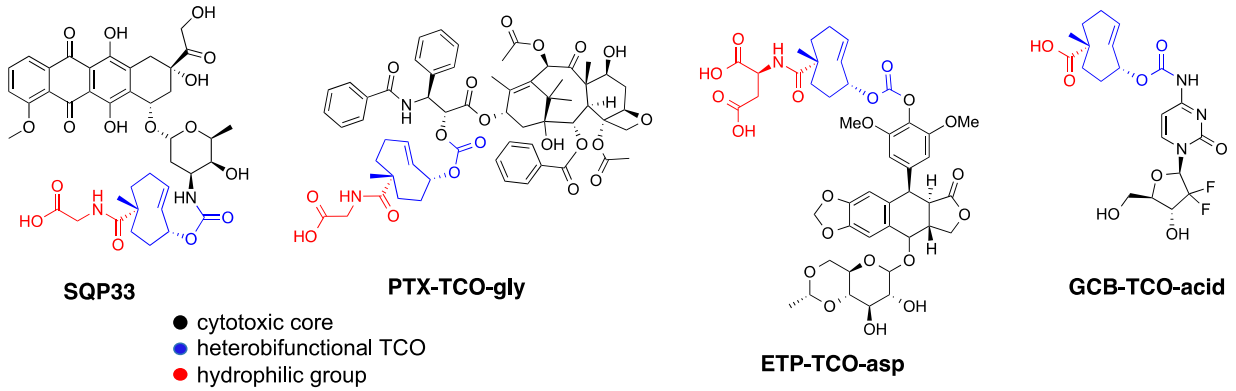

Scheme 1. Chemical structures of TCO-protodrugs of various cytotoxics.

The first synthetic strategy, utilized for the synthesis of Dox protodrug SQP33, entailed sequential coupling of the drug followed by the hydrophilic group to heterobifunctional TCO

intermediate **1**. Derivative **1** was prepared as a single diastereomer in 11 steps starting from 1,5-cyclooctadiene.[24-25] The critical final steps are described in **Scheme 2**. Coupling of Dox to the more reactive NHS carbonate afforded compound **2**. The final step proved to be challenging, as the direct coupling of glycine proceeded in low yield. Alternatively, coupling of glycine methyl ester failed to offer a path forward due to the challenges of subsequent saponification given the lability of Dox to basic hydrolysis of the methyl ester. Enzymatic ester hydrolysis was also unsuccessful due to poor ester solubility in phosphate-buffered saline (PBS). Moreover, addition of dimethyl sulfoxide (DMSO) as a co-solvent interfered with the esterase activity. We also considered acid-labile protecting groups, but, recognized that the sensitivity of the TCO group towards isomerization to the corresponding *cis*-isomer mitigated against this strategy. Finally, we discovered that transient protection of the carboxylic acid moiety of glycine as a trimethylsilyl (TMS) ester allowed efficient coupling to **2**. The TMS protecting group was found to be extremely moisture-sensitive and its deprotection was achieved upon aqueous workup of the reaction mixture.

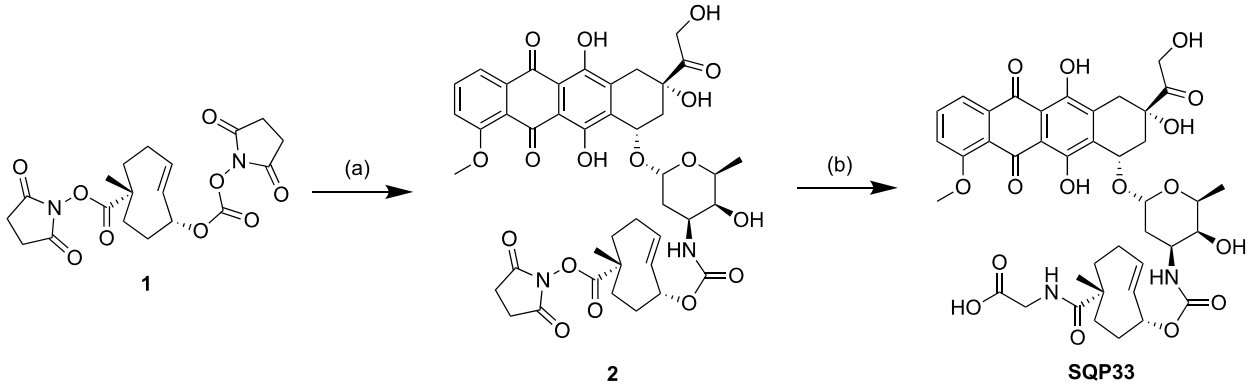

Scheme 2. Synthesis of SQP33: (a) Dox, DIPEA, DMF; (b) glycine, TMS-Cl, DIPEA, CH_2Cl_2, CH_3CN.

Two different synthetic strategies, illustrated in **Scheme 3A** and **3B**, were developed to synthesize the protodrugs of PTX and ETP. In each strategy, the heterobifunctional TCO derivative **3,** was first coupled to hydrophilic groups containing protected carboxylic acids. As shown in the preparation of the PTX protodrug in **Scheme 3A**, Fmoc-protected glycine ester **4** was prepared, activated to *p*-nitrophenyl carbonate **5**, and coupled with PTX at the side chain hydroxyl to give the Fmoc-protected intermediate **6**. Then, **PTX-TCO-gly** was obtained by removal of the Fmoc protecting group using piperidine in DMF. The preparation of the ETP protodrug is shown in **Scheme 3B**. Briefly, TCO derivative **3** was modified with bis-2-(trimethylsilyl)ethyl aspartate to give intermediate **8**, and the allylic alcohol group was converted to the *p*-nitrophenyl (PNP) carbonate **9**. **ETP-TCO-asp** was obtained by coupling of **9** with ETP and subsequent deprotection of the bis-(trimethylsilyl)ethyl ester groups using TBAF.

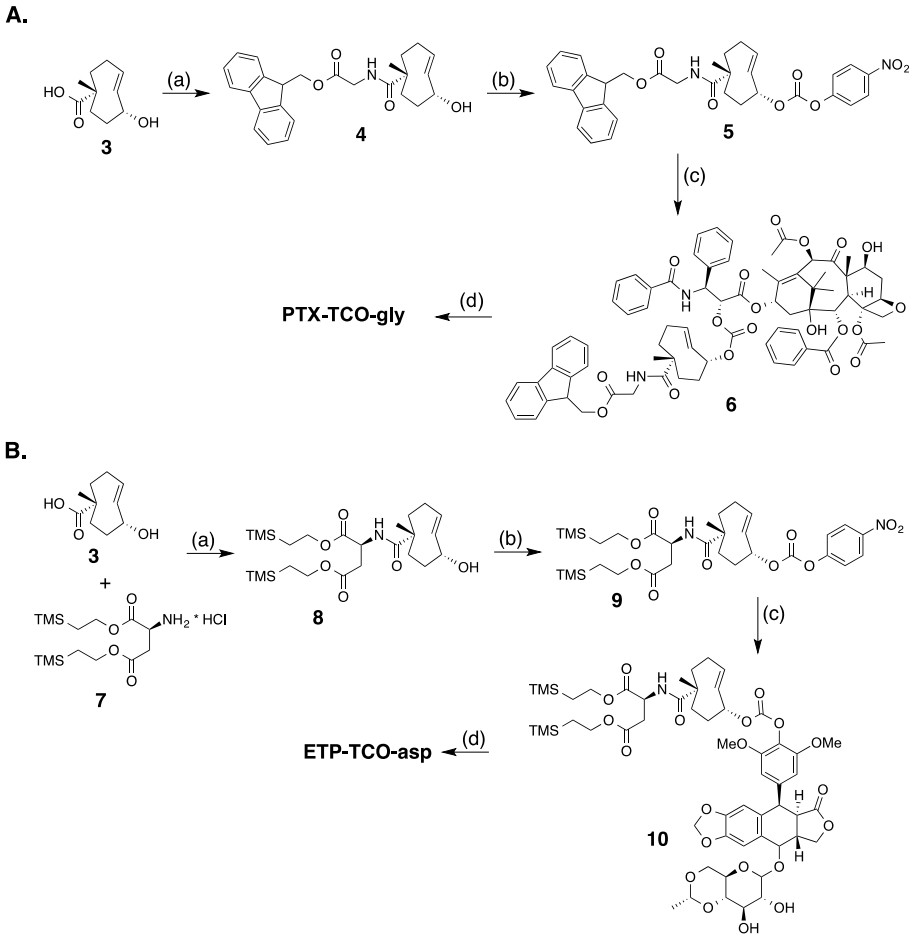

Scheme 3. (A) Synthesis of **PTX-TCO-gly**: (a) Fmoc-O-glycine, HATU, DIPEA, DMF; (b) PNP-Cl, pyridine, CH_2Cl_2; (c) paclitaxel, DMAP, CH_2Cl_2; (d) piperidine, DMF. (B) Synthesis of **ETP-TCO-asp**: (a) HATU, DIPEA, DMF; (b) PNP-Cl, pyridine, CH_2Cl_2; (c) etoposide, Cs_2CO_3, DMF; (d) TBAF, THF.

A third synthetic strategy was employed to access **GCB-TCO-acid**, as illustrated in **Scheme 4**. First, the carboxylic acid group of the TCO **3** was protected in two steps: (1) selective conversion to NHS ester **11** using N,N-disuccinimidyl carbonate (DSC), followed by (2) coupling with to 2-(trimethylsilyl)ethanol to give TMS ethyl ether **12**. The allylic alcohol of **12** was subsequently converted into an active PNP carbonate, which reacted with the free amino group of tetraisopropyldisiloxane-protected gemcitabine **14** to give adduct **15**. Global deprotection of the silyl groups with TBAF afforded **GCB-TCO-acid.**

Extensive *in vitro* evaluation of the protodrugs was carried out to choose a suitable candidate for *in vivo* studies. The goal was to identify protodrugs that would be at least ten-fold less cytotoxic than the parent drugs, and which were up to ten-fold more soluble in physiologically-relevant aqueous media. Both of these factors would allow safe administration of higher systemic doses. The stability of each protodrug was also tested in mouse blood plasma to exclude the possibility of non-specific protodrug activation. Lastly, it was confirmed that a Tz-modified biopolymer could both efficiently capture the protodrugs, and subsequently activate them into the active cytotoxic drugs.

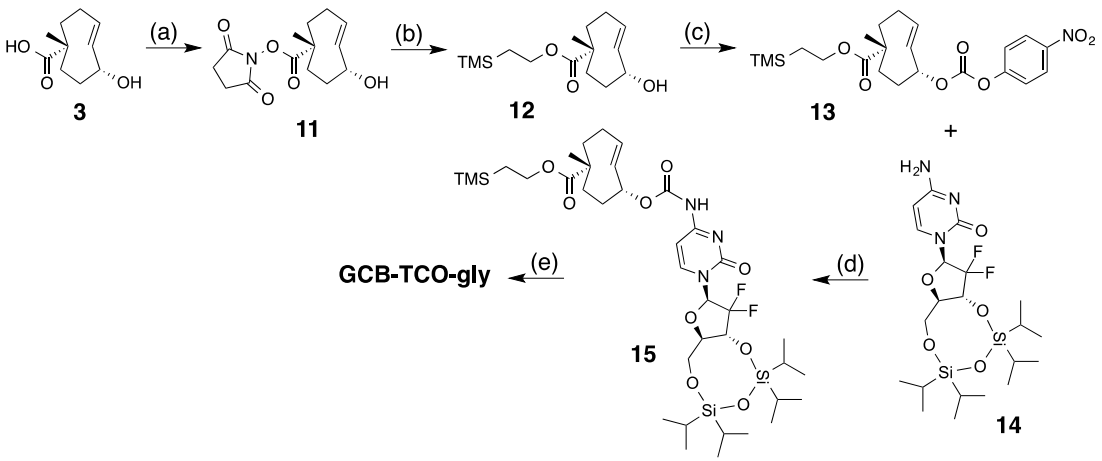

Scheme 4. Synthesis of **GCB-TCO-acid**: (a) DSC, DIPEA, CH_3CN; (b) TMS-ethanol, NaH, THF; (c) PNP-Cl, pyridine, CH_2Cl_2; (d) NaH, DMF; (e) TBAF, THF.

Table 1 summarizes cytotoxicity, solubility, plasma stability and biopolymer-triggered activation of the protodrugs. TCO modification resulted in a pronounced lowering of cytotoxicity of the protodrugs of Dox and ETP. Specifically, SQP33 was 83-times less cytotoxic to murine colorectal MC38 cells than Dox, while **ETP-TCO-asp** was 67-times less cytotoxic than ETP in this same assay. In contrast, we found more modest reductions in cytotoxicity, less than 10-fold reduction, for the protodrugs of PTX and GCB, suggesting that the pharmacophore might not be fully masked in those derivatives. In each case, the addition of the hydrophilic groups to the TCO moieties improved the solubility of each of the protodrugs, except for GCB, which is typically administered as an HCl salt. The most dramatic effect was again observed for SQP33, which was 7.3-times more soluble in PBS than the HCl salt of Dox. HPLC studies described in the supplementary information confirmed that Tz-modified biopolymer can efficiently convert the protodrugs of Dox, PTX and ETP into the corresponding active cytotoxic agents over a 24-hour (h) period. Activation of **GCB-TCO-acid** was studied using NMR. Based on these results, SQP33 and **ETP-TCO-asp** appeared to be the best candidates for *in vivo* studies. To focus on a single agent for preclinical studies suitable for enabling an Investigational New Drug (IND) application, SQP33 was chosen on the basis of its plasma stability.

Compound	Cytotoxicity (IC_{50})	Solubility in PBS (mg/mL)	Protodrug Plasma Stability (%)
Dox HCl	23 nM	3.8	
SQP33	1.9 μM (83-fold)	28	>99
PTX	32 nM	0.1	
PTX-TCO-gly	80 nM (2.5-fold)	1	96.5
ETP	160 nM	2.8	
ETP-TCO-asp	10.8 μM (67-fold)	5	65.8
GCB HCl	3 nM	38.6	
GCB-TCO-acid	26 nM (8.7-fold)	3	>99

Table 1. Summary of protodrug *in vitro* properties.

SQL70 Biopolymer

SQL70 biopolymer is based on the non-sulfated glycosaminoglycan, NaHA, that is well tolerated in the body, and has been used clinically in unmodified, crosslinked, and derivatized form for over five decades.[26-27] Commercially available NaHA was modified with Tz, as shown in **Scheme 5**. Briefly, NaHA was activated with NHS and the carbodiimide EDC-HCl in the presence of methyl tetrazine amine **16** in aqueous solution. Removal of reagents and byproducts by tangential flow filtration afforded the NaHA-Tz biopolymer. After assessment of different HA polymers and different degrees of Tz substitution, the NaHA-Tz biopolymer formed from 12-kDa HA and 19 weight% Tz modification was selected, henceforth called SQL70 biopolymer.

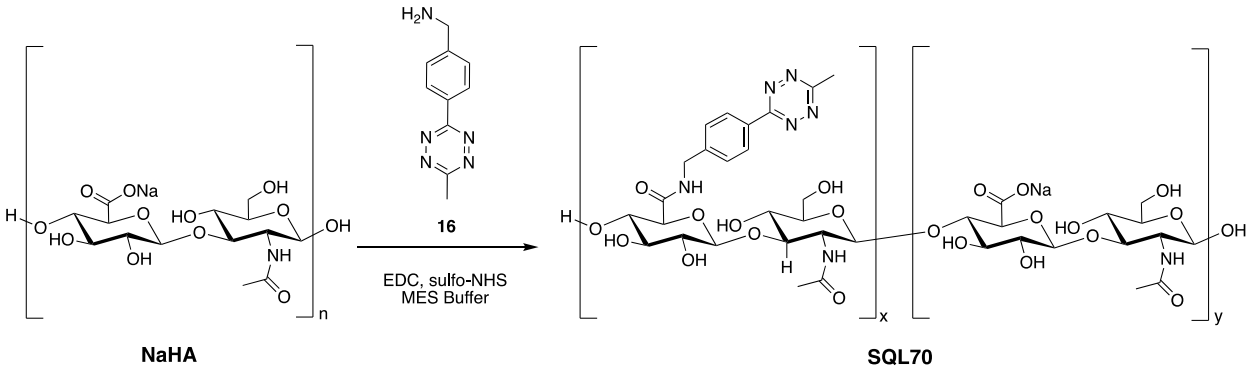

Scheme 5. Structure and synthetic scheme of SQL70 biopolymer.

In Vivo Pharmacokinetics and Reduced Systemic Toxicity of SQ3370

Studies in rodents were carried out to determine the plasma PK and tissue Dox exposure of treatment with SQ3370 as compared to conventional Dox HCl. Due to SQP33's enhanced solubility and reduced toxicity (83-fold less toxic than Dox HCl *in vitro*), rats injected subcutaneously with SQL70 could readily tolerate a cumulative IV dose of SQP33 equivalent to 10.8-times the cumulative MTD of Dox HCl, representing a significant safety margin over existing clinically-tested Dox-based therapeutics. **Figure 2** compares the amount of Dox safely administered in one week via SQ3370 to the multi-dose MTD administered over a month of conventional Dox HCl or Dox-based therapeutics that have undergone clinical evaluation. The tolerability of considerably higher doses in a shorter amount of time was attributed primarily to the attenuated systemic cytotoxicity of SQP33. Moreover, the ability of SQL70 biopolymer to efficiently sequester the protodrug out of circulation and concentrate the active Dox to a targeted site further contributed to higher dose tolerance. The efficiency of capture and activation *in* vivo were further investigated by PK analysis, as described below.

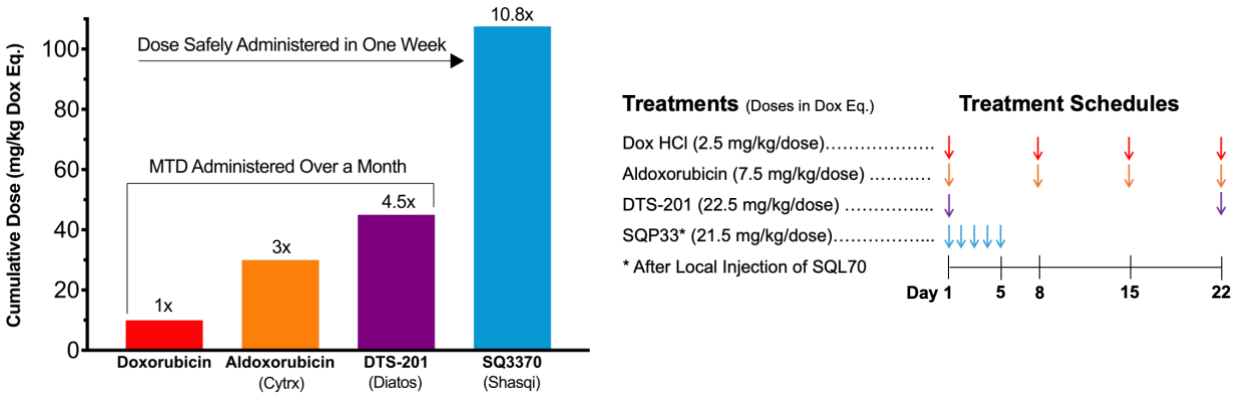

Figure 2. Tolerability of SQ3370 as compared to Dox and clinically-tested Dox-based treatments in rats. With SQ3370, over 21.5 mg/kg/dose of Dox was safely administered through 5 consecutive daily doses of SQP33 protodrug (cumulative 107.5 mg/kg) after an injection of SQL70 biopolymer. With conventional Dox, the MTD, administered over 4 weekly doses, is less than 10 times that amount,[28] and previous Dox-based treatments have only been able to advance the MTD up to 45 mg/kg administered in two doses 22 days apart.[29] All doses are represented in Dox HCl equivalents (Dox Eq).

SD rats were split into two groups, one group receiving a SC SQL70 biopolymer injection 1 h before start of SQP33 dosing, and the other group receiving only SQP33 protodrug infusions without an SQL70 biopolymer injection. SQP33 was administered IV to both groups on Days 1, 2, 3, 4 and 5 at 21.5 mg/kg/day in Dox Eq. Each daily dose of SQP33 was the equivalent of 2.9-times the single-dose MTD of Dox (7.4 mg/kg),[30] and the cumulative dose of SQP33 over the 5 days (107.5 mg/kg Dox Eq) was 10.8-times the multi-dose MTD of Dox given over 22 days (10 mg/kg),[28] as discussed previously. No adverse effects were observed in animals receiving these high doses throughout the study. Blood was drawn 0.5, 1, 2, 3, 4, 6, 8, 12 and 24 h post-SQP33 injection on each day and liquid chromatography–mass spectrometry (LC-MS) was used to measure plasma SQP33 protodrug and active Dox concentrations. Day 1 plasma concentrations of protodrug and active Dox, following a single dose of SQP33 in the absence or presence of SQL70 biopolymer are shown in **Figure 3**. When biopolymer was injected, within 30 minutes after dosing the plasma concentration of protodrug was below the limit of quantification (BLOQ; 1 ng/mL), indicating rapid capture by the biopolymer. This was associated with an increase in Dox, confirming release of the active drug. Conversely, in the absence of SQL70 biopolymer, the administered protodrug was detected throughout the 24 h period, with significantly lower levels of Dox detected. Comparison of PK parameters (**Tables S1 and S2**) in the absence and presence of SQL70 provide additional quantitative comparison. On Day 1, the plasma exposure of active Dox in the no-SQL70 group, as measured by area-under-the-curve (AUC), was only 2.2% of the value of the SQL70-injected group, suggesting that SQP33 protodrug was stable *in vivo* with minimal non-specific conversion to active Dox in the absence of SQL70 biopolymer. Accordingly, the Day 1 plasma exposure of SQP33 protodrug decreased by 2,444-fold in the presence of SQL70 (compared to the no-SQL70 group), as rapid capture by the biopolymer rendered the protodrug undetectable in plasma following the 0.5 h timepoint.

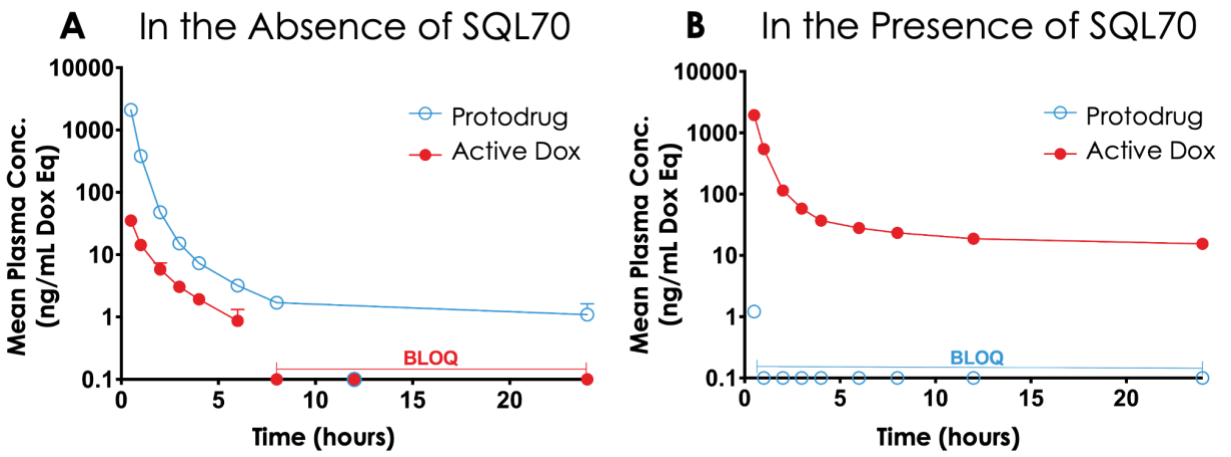

Figure 3. Nonspecific activation of SQP33 protodrug. SD Rats were treated with an intravenous infusion of SQP33 protodrug at 21.5 mg/kg Dox Eq (2.9-times higher than the single-dose MTD of Dox HCl) in the absence (A) or presence (B) of SQL70 biopolymer (click activating group) injection. This figure shows the 24 h plasma concentrations of SQP33 protodrug and active Dox following treatment. Plasma concentrations of SQP33 protodrug and active Dox were measured using LC-MS at 0.5, 1, 2, 3, 4, 6, 8, 12, and 24 h after the SQP33 protodrug infusion. Concentrations are displayed on a $\log_{10}$ scale of the mean + SEM of n=3 per timepoint.

PK analysis also showed SQL70 biopolymer retains *in vivo* activity over the 5-day dosing period. The plasma concentrations of SQP33 protodrug and active Dox over the 5-day SQP33 dosing period following a single SQL70 biopolymer injection on Day 1 are shown in **Figure 4**. An increase in the plasma concentration of active Dox was observed (compared to the no biopolymer control on Day 1) following each dose of SQP33 when SQL70 biopolymer was present, indicating a retention of the activating capabilities over the 5-day treatment period. We note that the maximum concentration (C_{max}) of SQP33 protodrug increased with each additional dose, while the C_{max} of active Dox decreased over the 5 days (**Table S2**). The average plasma SQP33 protodrug C_{max} on Day 5 with SQL70 biopolymer (**Table S2**) was reduced by 289.7 ng/mL compared with the average C_{max} (**Table S1**) of the no-biopolymer treatment group from Day 1 to Day 5. This finding was correlated with a 74.9 ng/mL increase in the average plasma active Dox C_{max} on Day 5 with SQL70 biopolymer (**Table S2**) compared to the average without the biopolymer (**Table S1**). This indicates that while activity is indeed retained over at least 5 days, there is a gradual decrease in the capture and activation properties. We hypothesize that this is due to multiple factors, including depletion of the number of active Tz sites on the biopolymer with repeated protodrug dosing, biopolymer clearance, or degradation of the Tz itself over time *in vivo*. Experiments in which a single dose of SQP33 was administered following SQL70 injection, with varying time intervals in between (**Figure S5**) show that activity diminishes even without repeated protodrug dosing, suggesting that Tz depletion is not the only factor.

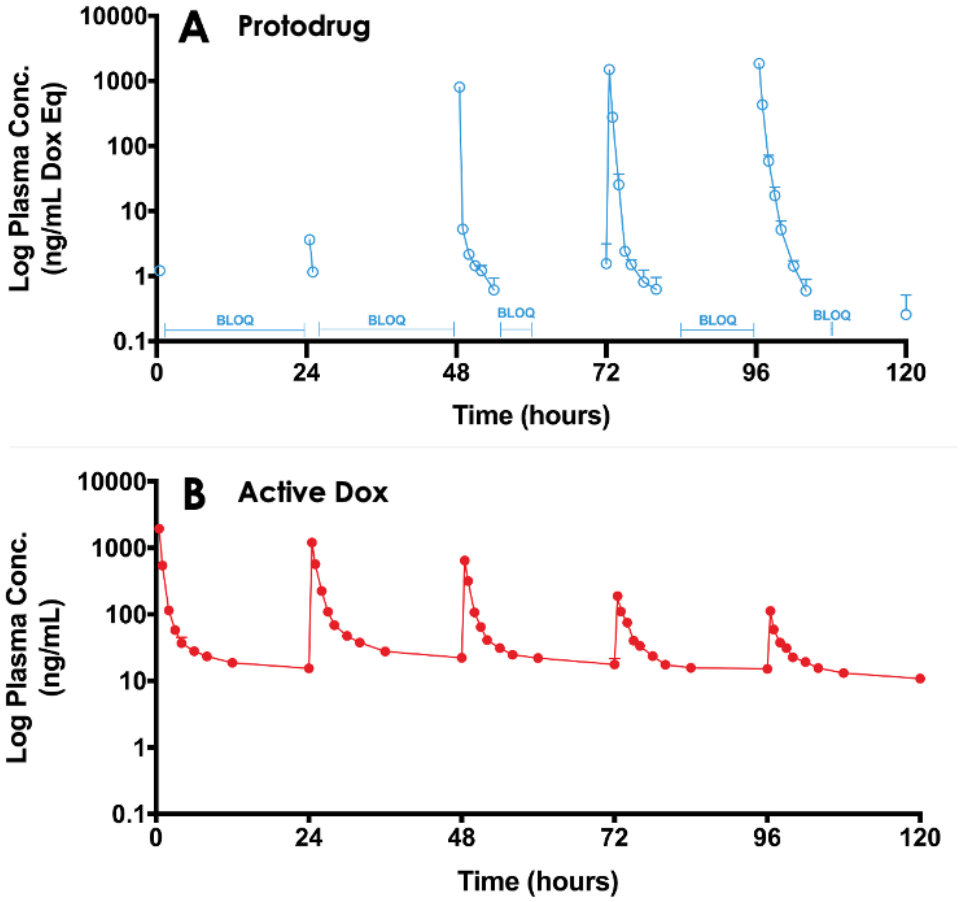

Figure 4. 5-day plasma concentration-time curves of SQP33 protodrug and active Dox in rats treated with SQ3370. SD rats were given one SC SQL70 biopolymer injection 1 h before SQP33 protodrug dosing began. 21.5 mg/kg/dose Dox Eq of SQP33 protodrug was administered IV at time points 0, 24, 48, 72, and 96 h. The cumulative dose of SQP33 protodrug added up to 107.5 mg/kg Dox Eq (10.8-times higher than the multi-dose MTD of Dox HCl). Plasma concentrations of SQP33 protodrug and active Dox were measured using LC-MS at 0.5, 1, 2, 3, 4, 6, 8, 12, and 24 h after each SQP33 protodrug dose. Plasma concentrations over 120 h are displayed on a $\log_{10}$ scale of the mean + SEM of n=3 per timepoint for both SQP33 protodrug (A) and active Dox (B). Plasma SQP33 protodrug curve (A) is disconnected between some measurements because concentrations between those measurements were BLOQ (1 ng/mL).

To explore the off-target active drug exposure of the CAPAC platform compared to conventional chemotherapy, we compared the tissue active Dox exposure from treatment with SQ3370 to that of treatment with conventional Dox HCl. Two groups of SD rats were treated with 5 daily doses SQP33 at 21.5 mg/kg/dose Dox Eq in the presence or absence of SQL70 biopolymer and compared to a control group that was injected IV with Dox HCl at 8.1 mg/kg. Tissue samples were collected from the heart, kidney and liver 5 days after treatment, and analyzed using LC-MS. **Figure 5** shows the dose-adjusted tissue active Dox exposure for each group. In both groups that were treated with SQP33, adverse active Dox exposure to non-target tissues was significantly lower than the group treated with conventional Dox HCl. Importantly, the heart Dox exposure was significantly lower in SQ3370 treatment, which may result in a reduction of Dox-induced cardiotoxicity.

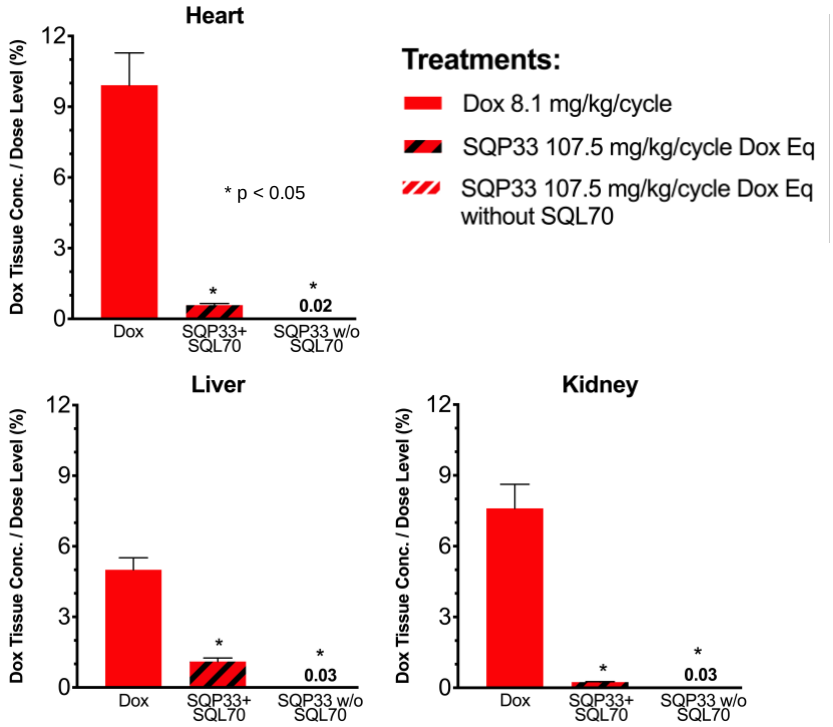

Figure 5. Active Dox exposure to non-target-tissues in SQ3370 vs. conventional Dox HCl. SD rats (n=3-5 per group) were treated with one dose of Dox HCl, at 8.1 mg/kg, and compared to rats treated with 5 daily doses of SQP33, at 21.5 mg/kg/dose Dox Eq, in the presence (+) or absence (w/o) of SQL70 biopolymer. Tissue samples were collected from the heart, kidney and liver 5 days after treatment, and analyzed using LC-MS. Tissue exposure is reported as a percent of the cumulative Dox Eq dose that was administered. Significance was established by unpaired t-test with Welch's correction. Data shows group mean + SEM. Active Dox exposure to non-target-tissues was significantly lower with SQ3370 treatment as compared to Dox HCl treatment.

Lastly, we examined the PK and biodistribution of a protodrug dosing regimen longer than 5 days. Healthy female C57BL/6 mice were treated with a single SC biopolymer injection followed by 15 IV infusions of SQP33 protodrug at 43 mg/kg/dose Dox Eq into the tail vein over 3 weeks (5 daily doses per week on weekdays only). The dosage schedule is shown in **Figure S6A**. Blood samples were collected at 1 h (n = 3), 24 h (n = 2), and on Days 5, 12, and 19 (n = 5) following the first SQP33 protodrug injection. Biopolymer injection site tissue was collected on Days 19 (n = 1) and 26 (n = 4). Samples were analyzed by LC-MS for SQP33 protodrug and active Dox, and are shown in **Figure S6B**, **C** and **D**, for plasma and targeted region (biopolymer injection site), respectively.

Consistent with results in rats, SQP33 was rapidly captured by the biopolymer on the first day of dosing. 1 h after the first SQP33 protodrug dose, plasma concentrations were almost exclusively active Dox, indicating efficient protodrug capture and activation. Within 24 h, there was no detectable SQP33 protodrug in plasma, and reduced levels of active Dox were observed compared with the 1 h time point - suggesting clearance of active Dox. Plasma analyses on Days 5, 12, and 19 showed increasing amounts of SQP33 protodrug 1 h after the infusion. Conversely, plasma concentrations of active Dox decreased over the treatment course from 1257 ng/mL on Day 1 to 73.5 ng/mL on Day 5 and down to 37.7 ng/mL on Day 12. These trends are similar to those seen in rats and indicate the biopolymer activity gradually decreases over time *in vivo*.

Results from this experiment also show that on the last day of SQP33 protodrug dosing (Day 19), the average concentration of active Dox in plasma was much smaller than that of

SQP33**;** while, in notable contrast, concentration of active Dox at the biopolymer injection site was markedly higher than that of SQP33 (**Figure S6C**, **Table S3**). Furthermore, on Day 26, 7 days after the final SQP33 dose, no SQP33 protodrug was detected at the targeted site, while active Dox levels were still more than 51% of the biopolymer injection site active Dox levels detected on Day 19 (**Figure S6D**, **Table S3**). Taken together, these results show a higher active drug exposure at the targeted region, as compared to plasma, and indicate that a detectable amount of active Dox remains at the biopolymer injection site for at least 7 days after the last SQP33 protodrug dose.

Conclusions

We have described studies directed at the selection and preclinical development for targeted activation of systemically administered anticancer protodrugs using click chemistry. The CAPAC platform addresses critical limitations of conventional chemotherapy and targeted delivery approaches. Synthesis and *in vitro* evaluation of protodrugs of Dox, PTX, ETP and GCB have been described. The protodrug of Dox, SQP33, was found to be 83-times less cytotoxic than the parent drug and 7.3-times more soluble in PBS and was therefore selected as the best candidate for *in vivo* testing. SQP33 was found to be stable in plasma and was efficiently activated by a Tz-modified biopolymer. After injection of SQL70 biopolymer, SD rats tolerated cumulative SQP33 doses 10.8-times higher than the multi-dose MTD of Dox HCl, with each single dose of SQP33 equivalent to over 2.9-times the single-dose MTD of Dox HCl, making SQ3370 treatment notably less toxic than other clinically tested Dox-based therapeutics. Furthermore, SQ3370 showed significantly lower Dox exposure to the heart, thus, significantly diminishing the biggest limitation of treatment with conventional Dox HCl, and expanding the drug's therapeutic potential by allowing remarkably higher doses to be safely administered. The considerably wider therapeutic window of SQ3370 has been attributed to the greatly reduced systemic cytotoxicity of SQP33 protodrug combined with the ability of SQL70 biopolymer to effectively capture protodrug and concentrate it at a targeted site, and release active Dox locally – as shown by PK studies in mice and rats. Moreover, SQL70 biopolymer was shown to activate multiple IV doses of SQP33, allowing repeated dosing while maintaining a wide therapeutic window. Furthermore, the protodrug proved stable *in vivo*, with minimal nonspecific conversion. The encouraging results presented herein have paved way for the clinical development of SQ3370. A first-in-human Phase I clinical trial of SQ3370 has been approved by the FDA and is currently enrolling patients with advanced solid tumors (ClinicalTrials.gov ID: NCT04106492).

References

1. Li, C.; Yu, D. F.; Inoue, T.; Yang, D. J.; Tansey, W.; Liu, C. W.; Milas, L.; Hunter, N. R.; Kim, E. E.; Wallace, S., Synthesis, biodistribution and imaging properties of indium-111-DTPA-paclitaxel in mice bearing mammary tumors. *J. Nucl. Med.* **1997,** *38* (7), 1042-7.
2. Cooley, T.; Henry, D.; Tonda, M.; Sun, S.; O'Connell, M.; Rackoff, W., A randomized, double-blind study of pegylated liposomal doxorubicin for the treatment of AIDS-related Kaposi's sarcoma. *Oncologist,* **2007,** *12* (1), 114-23.
3. Jain, D., Cardiotoxicity of doxorubicin and other anthracycline derivatives. *J. Nucl. Cardiol.* **2000,** *7* (1), 53-62.
4. Lefrak, E. A.; Pitha, J.; Rosenheim, S.; Gottlieb, J. A., A clinicopathologic analysis of adriamycin cardiotoxicity. *Cancer,* **1973,** *32* (2), 302-14.
5. Quintana, R. A.; Banchs, J.; Gupta, R.; Lin, H. Y.; Raj, S. D.; Conley, A.; Ravi, V.; Araujo, D.; Benjamin, R. S.; Patel, S.; Vadhan-Raj, S.; Somaiah, N., Early Evidence of Cardiotoxicity and Tumor Response in Patients with Sarcomas after High Cumulative Dose Doxorubicin Given as a Continuous Infusion. *Sarcoma,* **2017,** *2017*, 7495914.
6. Mita, M. M.; Natale, R. B.; Wolin, E. M.; Laabs, B.; Dinh, H.; Wieland, S.; Levitt, D. J.; Mita, A. C., Pharmacokinetic study of aldoxorubicin in patients with solid tumors. *Invest. New Drugs,* **2015,** *33* (2), 341-8.
7. Tap, W. D.; Papai, Z.; Van Tine, B. A.; Attia, S.; Ganjoo, K. N.; Jones, R. L.; Schuetze, S.; Reed, D.; Chawla, S. P.; Riedel, R. F.; Krarup-Hansen, A.; Toulmonde, M.; Ray-Coquard, I.; Hohenberger, P.; Grignani, G.; Cranmer, L. D.; Okuno, S.; Agulnik, M.; Read, W.; Ryan, C. W.; Alcindor, T.; Del Muro, X. F. G.; Budd, G. T.; Tawbi, H.; Pearce, T.; Kroll, S.; Reinke, D. K.; Schoffski, P., Doxorubicin plus evofosfamide versus doxorubicin alone in locally advanced, unresectable or metastatic soft-tissue sarcoma (TH CR-406/SARC021): an international, multicentre, open-label, randomised phase 3 trial. *Lancet. Oncol.* **2017,** *18* (8), 1089-1103.
8. Schoffski, P.; Delord, J. P.; Brain, E.; Robert, J.; Dumez, H.; Gasmi, J.; Trouet, A., First-in-man phase I study assessing the safety and pharmacokinetics of a 1-hour intravenous infusion of the doxorubicin prodrug DTS-201 every 3 weeks in patients with advanced or metastatic solid tumours. *Eur. J. Cancer.* **2017,** *86*, 240-247.
9. DeFeo-Jones, D.; Brady, S. F.; Feng, D. M.; Wong, B. K.; Bolyar, T.; Haskell, K.; Kiefer, D. M.; Leander, K.; McAvoy, E.; Lumma, P.; Pawluczyk, J. M.; Wai, J.; Motzel, S. L.; Keenan, K.; Van Zwieten, M.; Lin, J. H.; Garsky, V. M.; Freidinger, R.; Oliff, A.; Jones, R. E., A prostate-specific antigen (PSA)-activated vinblastine prodrug selectively kills PSA-secreting cells in vivo. *Mol. Cancer Ther.* **2002,** *1* (7), 451-9.
10. DeFeo-Jones, D.; Garsky, V. M.; Wong, B. K.; Feng, D. M.; Bolyar, T.; Haskell, K.; Kiefer, D. M.; Leander, K.; McAvoy, E.; Lumma, P.; Wai, J.; Senderak, E. T.; Motzel, S. L.; Keenan, K.; Van Zwieten, M.; Lin, J. H.; Freidinger, R.; Huff, J.; Oliff, A.; Jones, R. E., A peptide-doxorubicin 'prodrug' activated by prostate-specific antigen selectively kills prostate tumor cells positive for prostate-specific antigen in vivo. *Nat. Med.* **2000,** *6* (11), 1248-52.
11. DiPaola, R. S.; Rinehart, J.; Nemunaitis, J.; Ebbinghaus, S.; Rubin, E.; Capanna, T.; Ciardella, M.; Doyle-Lindrud, S.; Goodwin, S.; Fontaine, M.; Adams, N.; Williams, A.; Schwartz, M.; Winchell, G.; Wickersham, K.; Deutsch, P.; Yao, S. L., Characterization of a novel prostate-specific antigen-activated peptide-doxorubicin conjugate in patients with prostate cancer. *J. Clin. Oncol.* **2002,** *20* (7), 1874-9.
12. Albright, C. F.; Graciani, N.; Han, W.; Yue, E.; Stein, R.; Lai, Z.; Diamond, M.; Dowling, R.; Grimminger, L.; Zhang, S. Y.; Behrens, D.; Musselman, A.; Bruckner, R.; Zhang, M.; Jiang, X.; Hu, D.; Higley, A.; Dimeo, S.; Rafalski, M.; Mandlekar, S.; Car, B.; Yeleswaram, S.; Stern, A.; Copeland, R. A.; Combs, A.; Seitz, S. P.; Trainor, G. L.; Taub, R.; Huang, P.; Oliff, A., Matrix metalloproteinase-activated doxorubicin prodrugs inhibit HT1080 xenograft growth better than doxorubicin with less toxicity. *Mol. Cancer Ther.* **2005,** *4* (5), 751-60.

13. de Weger, V. A.; Beijnen, J. H.; Schellens, J. H., Cellular and clinical pharmacology of the taxanes docetaxel and paclitaxel--a review. *Anticancer Drugs,* **2014,** *25* (5), 488-94.
14. Gelderblom, H.; Verweij, J.; Nooter, K.; Sparreboom, A., Cremophor EL: the drawbacks and advantages of vehicle selection for drug formulation. *Eur. J. Cancer,* **2001,** *37* (13), 1590-8.
15. Weiss, R. B.; Donehower, R. C.; Wiernik, P. H.; Ohnuma, T.; Gralla, R. J.; Trump, D. L.; Baker, J. R., Jr.; Van Echo, D. A.; Von Hoff, D. D.; Leyland-Jones, B., Hypersensitivity reactions from taxol. *J. Clin. Oncol.* **1990,** *8* (7), 1263-8.
16. Hande, K. R., Etoposide: four decades of development of a topoisomerase II inhibitor. *Eur. J. Cancer,* **1998,** *34* (10), 1514-21.
17. Reif, S.; Kingreen, D.; Kloft, C.; Grimm, J.; Siegert, W.; Schunack, W.; Jaehde, U., Bioequivalence investigation of high-dose etoposide and etoposide phosphate in lymphoma patients. *Cancer Chemother. Pharmacol.* **2001,** *48* (2), 134-40.
18. Chao, N.; Stein, A.; Long, G.; Negrin, R.; Amylon, M.; Wong, R.; Forman, S.; Blume, K., Busulfan/etoposide--initial experience with a new preparatory regimen for autologous bone marrow transplantation in patients with acute nonlymphoblastic leukemia. *Blood,* **1993,** *81* (2), 319-323.
19. Rossin, R.; Versteegen, R. M.; Wu, J.; Khasanov, A.; Wessels, H. J.; Steenbergen, E. J.; Ten Hoeve, W.; Janssen, H. M.; van Onzen, A.; Hudson, P. J.; Robillard, M. S., Chemically triggered drug release from an antibody-drug conjugate leads to potent antitumour activity in mice. *Nat. Commun.* **2018,** *9* (1), 1484.
20. Devaraj, N. K.; Thurber, G. M.; Keliher, E. J.; Marinelli, B.; Weissleder, R., Reactive polymer enables efficient in vivo bioorthogonal chemistry. *Proc. Natl. Acad. Sci.* **2012,** *109* (13), 4762-7.
21. Czuban, M.; Srinivasan, S.; Yee, N. A.; Agustin, E.; Koliszak, A.; Miller, E.; Khan, I.; Quinones, I.; Noory, H.; Motola, C.; Volkmer, R.; Di Luca, M.; Trampuz, A.; Royzen, M.; Mejia Oneto, J. M., Bio-Orthogonal Chemistry and Reloadable Biomaterial Enable Local Activation of Antibiotic Prodrugs and Enhance Treatments against Staphylococcus aureus Infections. *ACS Cent. Sci.* **2018,** *4* (12), 1624-1632.
22. Mejia Oneto, J. M.; Gupta, M.; Leach, J. K.; Lee, M.; Sutcliffe, J. L., Implantable biomaterial based on click chemistry for targeting small molecules. *Acta Biomater* **2014,** *10* (12), 5099-5105.
23. Mejia Oneto, J. M.; Khan, I.; Seebald, L.; Royzen, M., In Vivo Bioorthogonal Chemistry Enables Local Hydrogel and Systemic Pro-Drug To Treat Soft Tissue Sarcoma. *ACS Cent. Sci.* **2016,** *2* (7), 476-82.
24. Khan, I.; Seebald, L. M.; Robertson, N. M.; Yigit, M. V.; Royzen, M., Controlled in-cell activation of RNA therapeutics using bond-cleaving bio-orthogonal chemistry. *Chem. Sci.* **2017,** *8* (8), 5705-5712.
25. Robertson, N. M.; Yang, Y.; Khan, I.; LaMantia, V. E.; Royzen, M.; Yigit, M. V., Single-trigger dual-responsive nanoparticles for controllable and sequential prodrug activation. *Nanoscale,* **2017,** *9* (28), 10020-10030.
26. Prestwich, G. D., Hyaluronic acid-based clinical biomaterials derived for cell and molecule delivery in regenerative medicine. *J. Control. Release.* **2011,** *155* (2), 193-9.
27. Burdick, J. A.; Prestwich, G. D., Hyaluronic acid hydrogels for biomedical applications. *Adv. Mater.* **2011,** *23* (12), H41-56.
28. Kratz, F.; Ehling, G.; Kauffmann, H. M.; Unger, C., Acute and repeat-dose toxicity studies of the (6-maleimidocaproyl)hydrazone derivative of doxorubicin (DOXO-EMCH), an albumin-binding prodrug of the anticancer agent doxorubicin. *Hum. Exp. Toxicol.* **2007,** *26* (1), 19-35.
29. Ravel, D.; Dubois, V.; Quinonero, J.; Meyer-Losic, F.; Delord, J.; Rochaix, P.; Nicolazzi, C.; Ribes, F.; Mazerolles, C.; Assouly, E.; Vialatte, K.; Hor, I.; Kearsey, J.; Trouet, A., Preclinical toxicity, toxicokinetics, and antitumoral efficacy studies of DTS-201, a tumor-selective peptidic prodrug of doxorubicin. *Clin. Cancer Res.* **2008,** *14* (4), 1258-65.

30. Bertazzoli, C.; Rovero, C.; Ballerini, L.; Lux, B.; Balconi, F.; Antongiovanni, V.; Magrini, U., Experimental systemic toxicology of 4'-epidoxorubicin, a new, less cardiotoxic anthracycline antitumor agent. *Toxicol Appl Pharmacol* **1985,** *79* (3), 412-22.

SUPPORTING INFORMATION

Click Activated Protodrugs Against Cancer Increase the Therapeutic Potential of Chemotherapy through Local Capture and Activation

K. Wu[1], N. A. Yee[2*], S. Srinivasan[2], A. Mahmoodi[2], M. Zakharian[2], J. M. Mejia Oneto[2], M. Royzen[1]*

[*] Co-first authorship
[1] University at Albany, 1400 Washington Ave., LS-1136, Albany, NY 12222
[2] Shasqi, Inc., 665 3rd St., Suite 501, San Francisco, CA 94107

Table of Contents	**Page No.**

Materials and Methods

All chemicals were received from commercial sources and used without further purification. Chromatographic purifications of synthetic materials were conducted using SiliaSphere™ spherical silica gel with an average particle and pore size of 5 µm and 60 Å, respectively (Silicycle Inc, QC, Canada). Thin layer chromatography (TLC) was performed on SiliaPlate™ silica gel TLC plates with 250 µm thickness (Silicycle Inc, QC, Canada). Preparative TLC was performed using SiliaPlate™ silica gel TLC plates with 1000 µm thickness. Analytical HPLC was performed using Phenomenex Luna 5u C18 (2) analytical column (250 x 5 mm) using a gradient of CH_3CN (0.01% formic acid) in H_2O (0.01% formic acid). HRMS and LC-MS data was acquired using Agilent Technologies 6530 Q-TOF instrument. ^{1}H and ^{13}C NMR spectroscopy was performed on a Bruker NMR at 500 MHz (^{1}H) and 125 MHz (^{13}C). All ^{13}C NMR spectra were proton decoupled.

Cell culture. MC38 cells were purchased from ATCC (American Type Culture Collection, cat.# CRL-2638) and propagated in Dulbecco's modified Eagle's medium (DMEM) containing 5% fetal bovine serum (FBS), supplemented with 100 U/mL penicillin, and 100 µg/mL streptomycin at 37°C in a 5% CO_2 incubator.

Cell proliferation assay. The colorimetric MTT (3-(4, 5- dimethylthiazol-2-yl)-2, 5-diphenyltetrazolium bromide) assay protocol was used to evaluate proliferation of MC38 cells. On day one, 1×10^3 cells/well in 96-well plates in 100 µL DMEM were plated and incubated for 24 h. On day two, the medium was removed, and the cells were treated with variable concentrations of cytotoxic compounds. On day three, the medium was replaced with 100 µL of fresh medium and cells were incubated for additional 48h. On day five, the medium was removed, and cells were incubated with 100 µL of MTT solution (0.6 mg/mL in DMEM) per well. Cells were incubated in the dark for 4 h at 37 °C. At the end of the incubation, the MTT solution was then replaced with 100 µL of DMSO containing 4% aqueous ammonia per well and agitated for 30 minutes. The absorbance of the purple formazan was recorded using a BioTek Synergy HT multi detection microplate reader at 550 nm. Results were generated from triplicate experiments.

Protodrug activation experiments. Protodrug activation experiments were carried out using Tz-modified alginate gel which has previously been described (*Acta Biomater.* **2014**,*10*, 5099-5105). This material was chosen because of the previously established protodrug activation protocol (*ACS Cent. Sci*. **2018**, *4*, 1624-1632). In particular, the crosslinked hydrogel provides an easy way for separation of small molecules from the biopolymer using centrifugation. The Tz-modified alginate gel (160 µL) was crosslinked using a supersaturated solution of $CaSO_4$ (40 µL) and placed inside of amicon 3K spin columns and treated with 5 nmol of protodrugs of DOX, PTX and ETP in 400 µL of PBS. After 2 h, the supernatant fractions were collected centrifugation at 6,000 RPM and Tz-modified alginate was resuspended in fresh PBS (400 µL). The supernatants were collected after 4, 6, and 24 h to monitor continuous drug release. The supernatant fractions were analyzed by HPLC. All kinetic experiments were carried out in triplicate. Activation of GCB-TCO-acid could not be done using this method because of the sensitivity of GCB to $CaSO_4$. Instead, we performed a ^{1}H NMR experiment where the protodrug was treated with a model Tz compound (3,6-Diisopropyl-1,2,4,5-tetrazine) and the spectra were recorded at different time intervals.

Protodrug plasma stability studies. Mouse blood plasma was purchased from BioIVT (Westbury, NY). Prepared 100 µM protodrug stock solutions in DMSO. Added 2 µL of a protodrug stock solution to 198 µL of mouse plasma and incubated at 37 °C. At different timepoints, 30 µL aliquots were diluted with 60 µL of ice cold Internal Standard Solution (acetonitrile containing 12.5 ng/mL of diclofenac) and mixed. Samples were centrifuged at 6,000g for 30 minutes and subsequently analyzed by LC-MS in the negative mode.

Dox Equivalence Calculations. The molecular weights (MW) of SQP33 (free acid form) and Dox hydrochloride (Dox HCl) are 810.81 g/mol and 579.98 g/mol respectively. SQP33 is composed of TCO-modified Dox. Thus, the molar conversion factor of SQP33 to Dox HCl is 0.7153, based on the MW ratios. All SQP33 protodrug values that were measured in plasma or administered as the dose in the studies reported here have been converted to Dox equivalents (Dox Eq) for a clear comparison of the amount of Dox delivered.

Pharmacokinetics and non-target tissue exposure in rats.

Study Design

Male *Sprague Dawley* (SD) rats were placed in 7 groups. Group 1 (n = 3) served as control and received a single intravenous (IV) dose of Dox HCl at 8.1 mg/kg. Group 2 (n = 3) evaluated SQP33's activity in the absence of SQL70 biopolymer, and received a single IV dose of SQP33, at 43 mg/kg Dox Eq, without a prior SQL70 biopolymer injection. Groups 3-5 (n = 3 per group) assessed the effect of elapsed-time between SQL70 biopolymer injection and SQP33 protodrug IV administration on SQ3370's local activation capacity. These groups received a single IV dose of SQP33 at 1 hour (group 3), 24 hours (group 4), or 96 hours (group 5) after a SC SQL70 biopolymer injection. Group 6 (n = 6) determined the effects of multiple IV SQP33 doses following a single SC SQL70 biopolymer injection, and animals received 5 IV doses of SQP33. The first SQP33 dose was 1 hour after SQL70 biopolymer injection followed by 4 additional daily doses. Lastly, Group 7 (n = 6) evaluated multiple doses of SQP33 in the absence of SQL70 biopolymer. These animals received 5 daily IV doses of SQP33 without a prior SQL70 biopolymer injection.

Dosing Procedures

Group 1: 8.1 mg of Dox per kg of body weight was dissolved in saline. Once a concentration of 1.62 mg/mL was achieved, a total volume of 5 mL per kg of body weight was administered IV via the tail vein. Group 2: 60 mg of SQP33 per kg of body weight was dissolved in saline at pH 7.4, and sodium hydroxide was added dropwise until SQP33 fully dissolved. Once a concentration of 12 mg/mL was achieved, a total volume of 5 mL per kg of body weight was administered IV via the tail vein. Groups 3 to 5: 1 mL of SQL70 was SC injected at the dorsal flank. 60 mg of SQP33 per kg of body weight was dissolved in saline at pH 7.4, and sodium hydroxide was added dropwise until SQP33 fully dissolved. Once a concentration of 12 mg/mL was achieved, a total volume of 5 mL per kg of body weight was administered IV via the tail vein at 1, 24, or 96 hours after SQL70 injection. Group 7: 1 mL of SQL70 was SC injected at the dorsal flank. 30 mg of SQP33 per kg of body weight was dissolved in saline at pH 7.4, and sodium hydroxide was added dropwise until SQP33 fully dissolved. Once a concentration of 6 mg/mL was achieved, a total volume of 5 mL per kg of body weight was administered IV via the tail vein 1 hour after SQL70 injection. Four additional daily doses were given at 24, 48, 72, and 96 hours after the first dose. Group 8: 30 mg of SQP33 per kg of body weight was dissolved in saline at pH 7.4, and sodium hydroxide was added dropwise until SQP33 fully dissolved. Once a concentration of 6 mg/mL was achieved, a total volume of 5 mL per kg of body weight was administered IV via the tail vein 1 hour after SQL70 injection. Four additional daily doses were given at 24, 48, 72, and 96 hours after the first dose.

In Life Assessment

All animals had 200 µL of blood collected via jugular vein catheter at multiple time-points throughout the study. Groups 1-5 received blood-draws pretreatment, and at 0.5, 1, 2, 3, 4, 6, 8, 12, 24, 48, 72, 96, and 120 hours after Dox HCl or SQP33 IV dose. In groups 6 and 7, half of the animals (n = 3 per group) received blood-draws pretreatment, and at 0.5, 1, 2, 3, 4, 6, 8, 12, 24 (before second dose), 48 (before third dose), 72 (before fourth dose), 72.5, 73, 74, 75, 76, 78, 80, 84, 96 (before fifth dose), 120, 144, 168, 192, 216, 240 hours after first SQP33 dose, and the other half (n = 3 per group) received blood-draws pretreatment, and at 24 (before second dose), 48 (before third dose), 48.5, 49, 50, 51, 52, 54, 56, 60, 72 (before fourth dose), 96 (before fifth dose) 96.5, 97, 98, 99, 100, 102, 104, 108, 120, 144, 168, 192, 216, 240 h after first SQP33 dose.

The blood-draws for groups 6 and 7 were split in this manner to decrease the amount of blood drawn from each animal to a safe level. All animals were euthanized 120 h after their last IV dose (their only IV dose for groups 1-5). For groups 1, 6, and 7, tissue samples were collected from the liver, heart and kidney, and were homogenized in deionized water and the concentration of active Dox (for tissue and plasma) and SQP33 protodrug (for plasma only) was quantified by LC-MS.

Pharmacokinetics and target tissue exposure in mice.

Study Design

5 female C57BL/6 mice were treated with a 100 µL SC injection of Tz-modified NaHA biopolymer (prototype of SQL70 biopolymer) followed by 15 IV injections of SQP33 protodrug, at 43 mg/kg/dose Dox Eq, into the tail vein over 19 days (one dose per day on weekdays only).

Dosing Procedure

100 µL of Tz-modified NaHA biopolymer was injected SC. 60 mg of SQP33 per kg of body weight was dissolved in saline at pH 7.4, and sodium hydroxide was added dropwise until SQP33 fully dissolved. Once a concentration of 6 mg/mL was achieved, a total volume of 10 mL per kg of body weight was administered IV via the tail vein once a day, on weekdays only, for 15 doses.

In Life Assessment

20 µL of blood was collected at different time points following the first SQP33 protodrug injection. Timepoints were at 1 hour (n = 3), 24 hours (n = 2), and on Days 5, 12, and 19 (n = 5). Biopolymer injection site tissue was collected on Days 19 (n = 1) and 26 (n = 4) after animals were euthanized. Injection site tissue samples were homogenized in deionized water. Tissue and plasma concentration of active Dox and SQP33 protodrug was quantified by LC-MS.

Table S1. Plasma pharmacokinetic parameters of active Dox and SQP33 protodrug in rats treated with 5 doses of SQP33 without SQL70 biopolymer.

Day	Active Dox		SQP33 Protodrug	
	$AUC_{0.5-24\ h}$# (ng*h/mL)	**C_{max}# (ng/mL)**	**$AUC_{0.5-24\ h}$# (ng*h/mL)**	**C_{max}# (ng/mL)**
1	41.8 ± 6.9	35.2 ± 3.7	1418 ± 176	2095.8 ± 221.8
2	No data recorded	No data recorded	No data recorded	No data recorded
3	41.1 ± 5.4	32.0 ± 5.3	1584 ± 331	1981.4 ± 427
4	46.6 ± .6	41.6 ± 0.5	1297 ± 172.1	1955.2 ± 236
5	54.5 ± 10.6	42.1 ± 6.0	1778 ± 356.3	2517.9 ± 548.2
Avg	36.5	37.7	1519.3	2137.6

AUC = area under the concentration-time curve; Avg = average; C_{max} = maximum observed concentration (time of observing C_{max} = 30 minutes); Dox = doxorubicin; Dox Eq = doxorubicin hydrochloride equivalents; SEM = standard error of mean.
# AUCs were determined using the Riemann Sum method. AUC and C_{max} results show mean ± SEM.

Table S2. Plasma pharmacokinetic parameters of active Dox and SQP33 protodrug in rats treated with 5 doses of SQP33 after a SC SQL70 biopolymer injection.

Day	Active Dox			SQP33 Protodrug		
	C_{max}[#] (ng/mL)	$AUC_{0.5-24\ h}$[#] (ng*h/mL)	AUC $Ratio_1$[§]	C_{max}[#] (ng/mL)	$AUC_{0.5-24\ h}$[#] (ng*h/mL)	AUC $Ratio_2$[†]
1	1953.3 ± 241.8	1928 ± 104.2	47.0	1.2 ± 0.2	0.6 ± 0.0	2444
2	1206.7 ± 54.4	2015± 25.3	N/A	3.6 ± 0.4	2.7 ± 0.2	N/A
3	644.3 ± 73.4	1221 ± 24.6	29.8	805.4 ± 144.2	413.4 ± 72	3.83
4	190 ± 6.1	655.5 ± 31.2	14.1	1506.9 ± 76.4	1014± 47.5	1.3
5	112.7 ± 3.2	462.9 ± 25.5	8.5	1847.9 ± 263.0	1337 ± 198	1.3

AUC = area under the concentration-time curve; C_{max} = maximum observed concentration (time of observing C_{max} = 30 minutes); Dox = doxorubicin; Dox Eq = doxorubicin hydrochloride equivalents; SEM = standard error of mean.

[#] AUCs were determined using the Riemann Sum method. AUC and C_{max} results are shown as mean ± SEM in each group.

[§] $Ratio_1$ was calculated by: [AUC with SQL70 biopolymer (from this table) ÷ AUC without SQL70 biopolymer (from **Table S1**)].

[†] $Ratio_2$ was calculated by: [AUC without SQL70 biopolymer (from **Table S1**) ÷ AUC with SQL70 biopolymer (from this table)].

Table S3. Concentration of active Dox and SQP33 protodrug in plasma or biopolymer injection site in mice treated with 15 SQP33 protodrug doses following a SC biopolymer injection.

Day	Location	Active Dox Conc.	SQP33 Protodrug Conc.	Percent*
19	Plasma	36.2 ng/mL	1325.6 ng/mL	2.7%
19	Injection site	151 ng/g	4.17 ng/g	3621%
26	Injection site	77.5 ng/g	BLOQ	N/A

BLOQ = below limit of quantification; Conc = concentration; Dox = doxorubicin; N/A = not applicable.
* Percent active Dox calculated by [active Dox conc ÷ SQP33 protodrug conc] in the same location and on the same day.

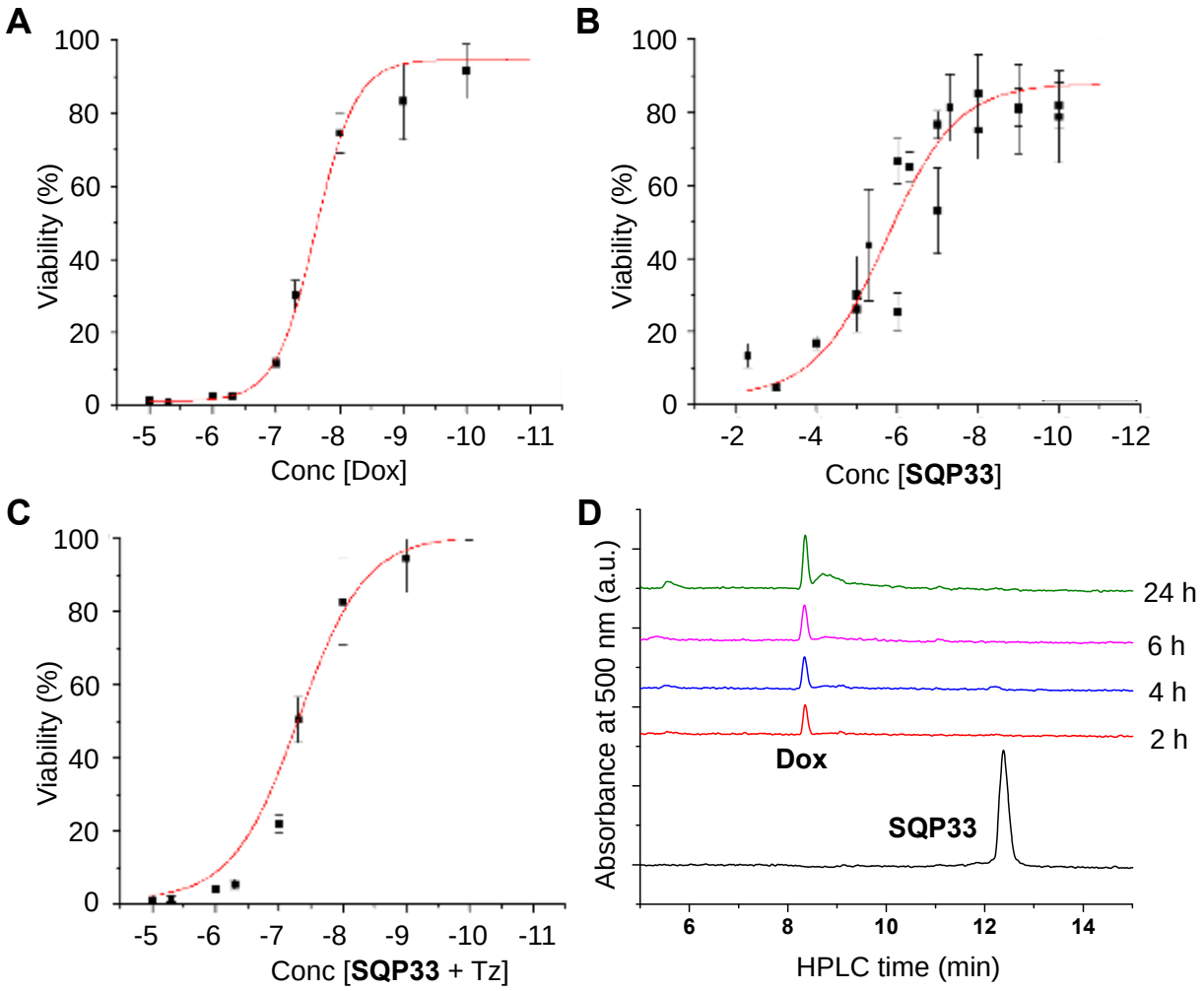

Figure S1. *In vitro* studies: (**A**) Viability of MC38 cells as a function of Dox concentration; (**B**) Viability of MC38 cells as a function of SQP33 concentration; (**C**) Viability of MC38 cells as a function of SQP33 + Tz concentration; (**D**) *in vitro* activation of SQP33 upon addition of the biopolymer.

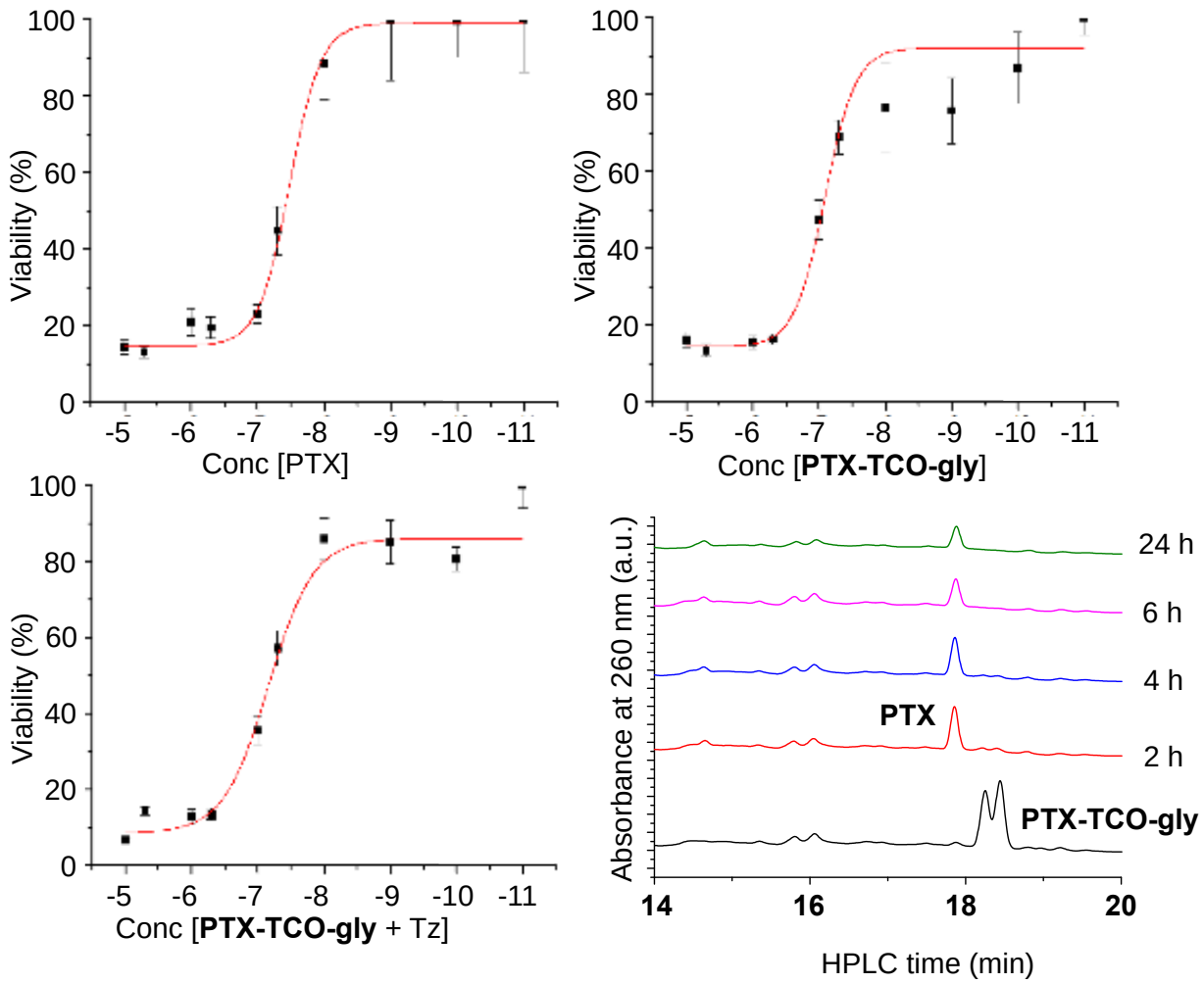

Figure S2. *In vitro* studies: (**A**) Viability of MC38 cells as a function of PTX concentration; (**B**) Viability of MC38 cells as a function of **PTX-TCO-gly** concentration; (**C**) Viability of MC38 cells as a function of **PTX-TCO-gly** + Tz concentration; (**D**) *in vitro* activation of **PTX-TCO-gly** upon addition of the biopolymer.

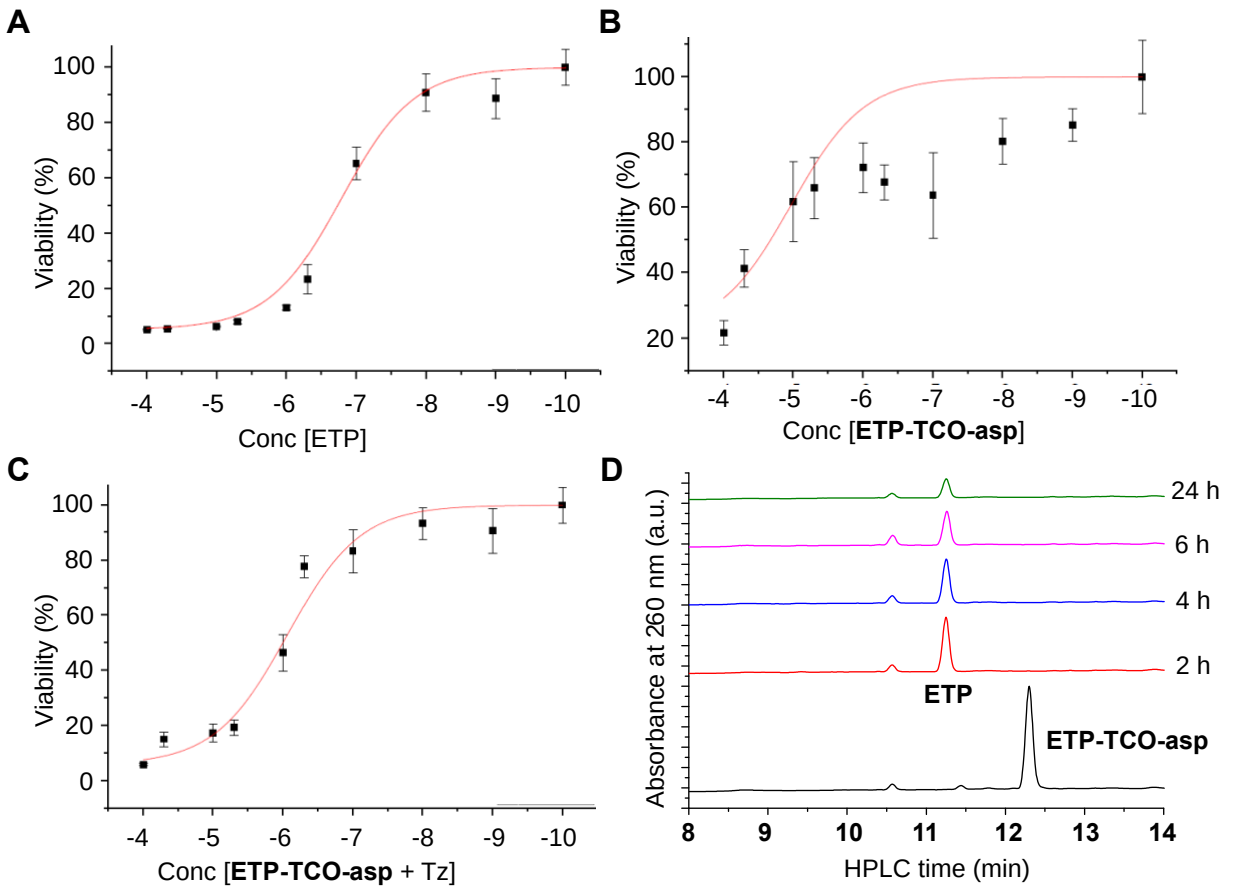

Figure S3. *In vitro* studies: (**A**) Viability of MC38 cells as a function of ETP concentration; (**B**) Viability of MC38 cells as a function of **ETP-TCO-asp** concentration; (**C**) Viability of MC38 cells as a function of **ETP-TCO-asp** + Tz concentration; (**D**) *in vitro* activation of **ETP-TCO-asp** upon addition of the biopolymer.

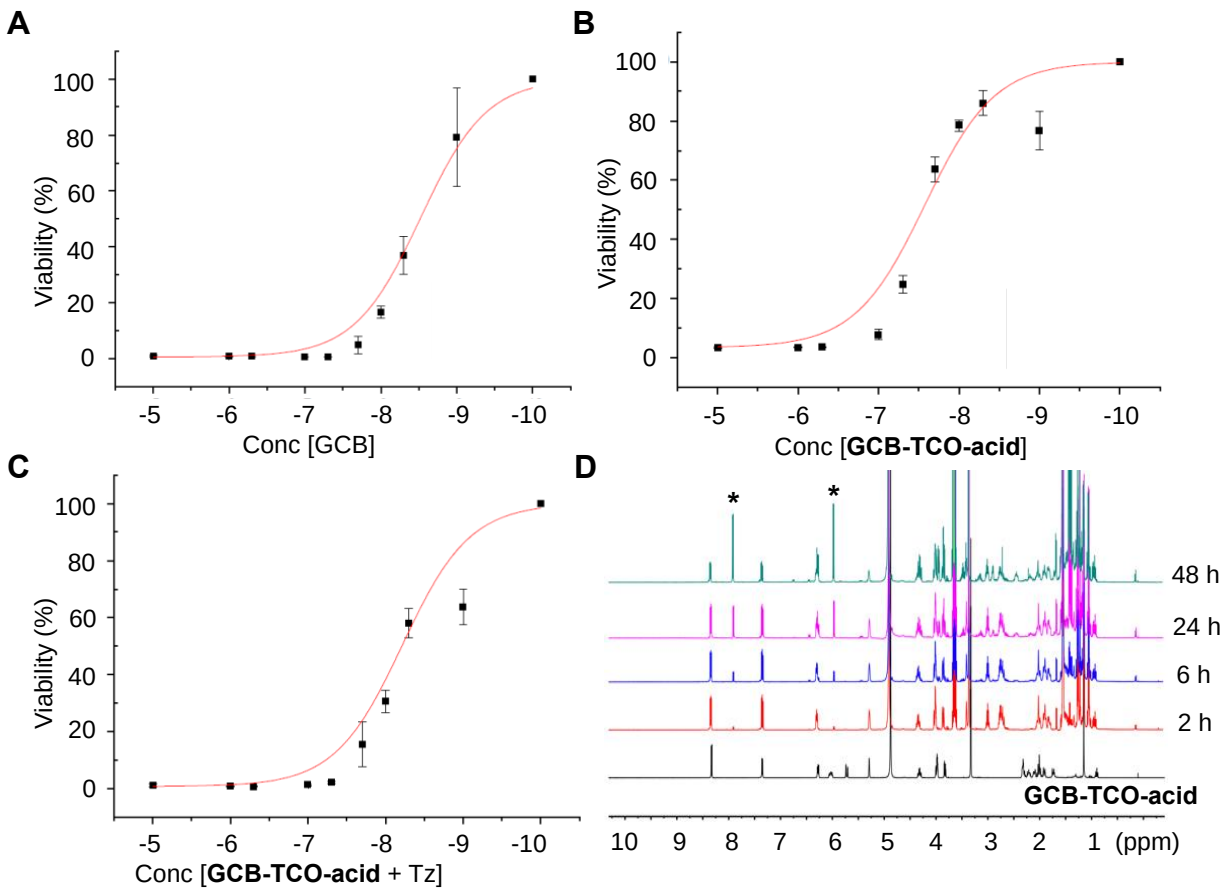

Figure S4. *In vitro* studies: (**A**) Viability of MC38 cells as a function of GCB concentration; (**B**) Viability of MC38 cells as a function of **GCB-TCO-acid** concentration; (**C**) Viability of MC38 cells as a function of **GCB-TCO-acid** + Tz concentration; (**D**) *in vitro* activation of **GCB-TCO-acid** upon addition of the biopolymer. Asterisks indicate the NMR signals corresponding to activated GCB.

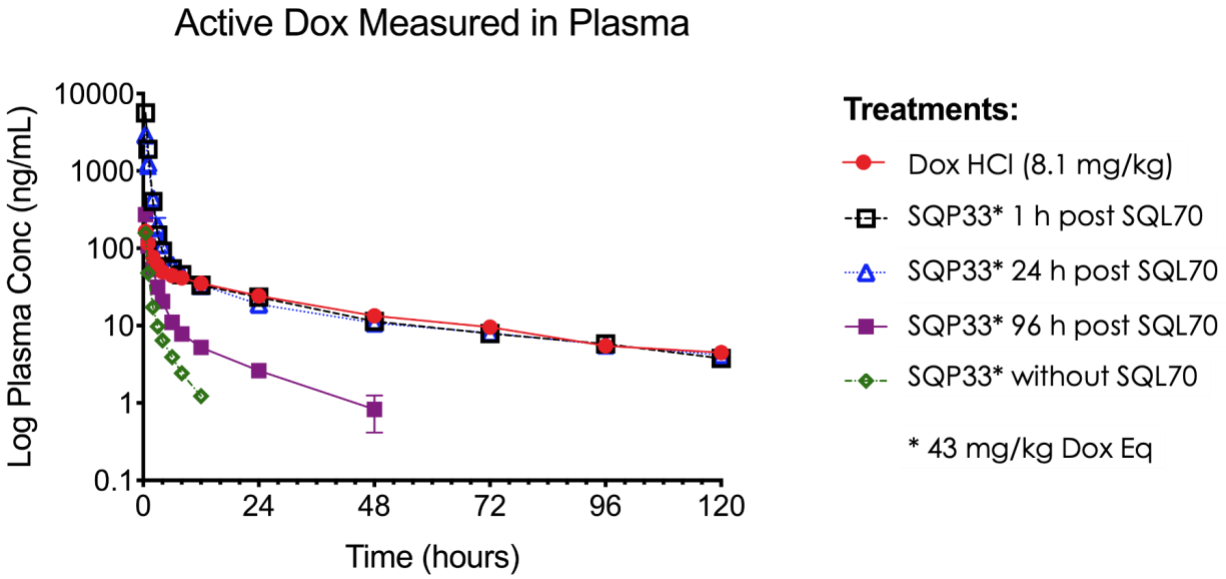

Figure S5. Sprague Dawley rats were treated with 1 IV dose of SQP33 protodrug, at 43 mg/kg Dox Eq, in the presence or absence of SC SQL70 biopolymer injection. SQP33 protodrug was administered at different timepoints post SQL70 injection for each group. Control animals were given 1 IV dose of Dox HCl at 8.1 mg/kg. Plasma samples were assessed for active Dox concentrations using LC-MS. Blood was drawn for analysis at 0.5, 1, 2, 3, 4, 6, 8, 12, 24, 48, 72, 96, and 120 hours following IV dose. Data is plotted as mean ± SEM for each group (n = 3). Plots end when the measurements following that time are BLOQ (1 ng/mL).

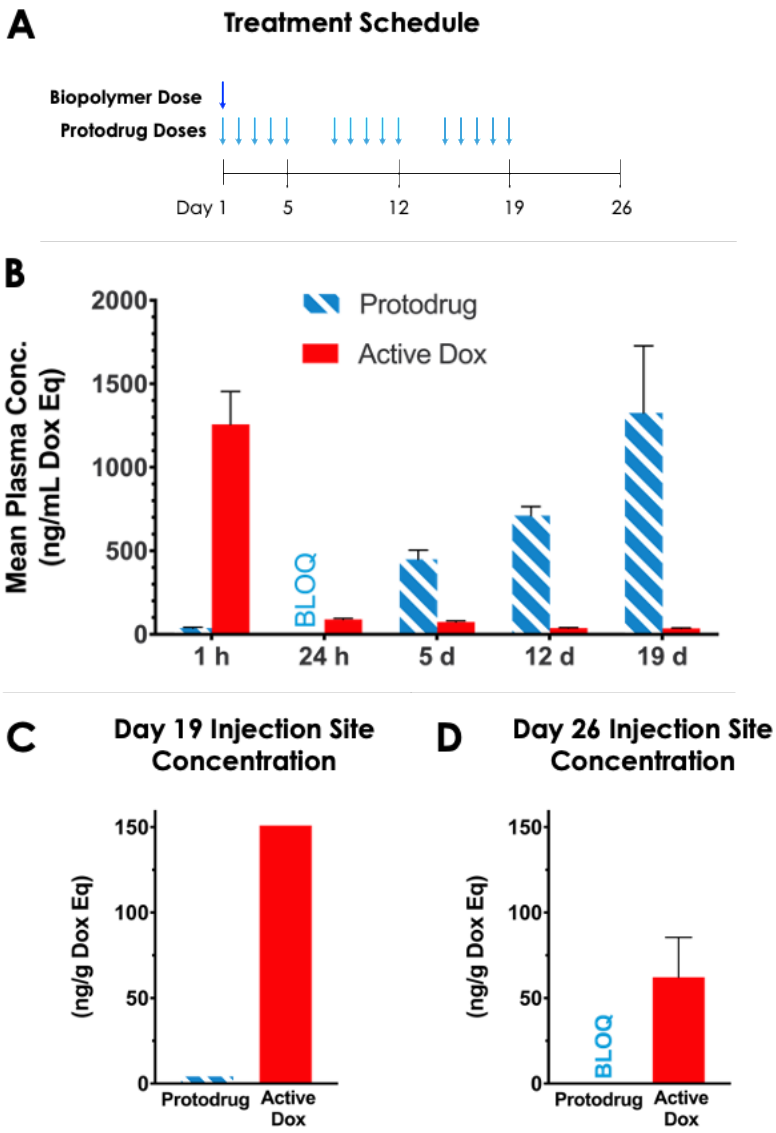

Figure S6. Plasma and biopolymer injection site (targeted region) concentrations of SQP33 protodrug and active Dox in mice. C57BL/6 mice (n = 5) received (A) one biopolymer injection followed by 15 SQP33 protodrug doses given over 19 days (5 daily doses per week, on weekdays only). Plasma was collected at 1 h, 24 h, Day 5, 12, and 19. Plasma concentrations of SQP33 protodrug and active Dox are shown in (B). At 1 h (on Day 19; n = 1) and 7 days (on Day 26; n = 4) after the last IV dose, tissue from the biopolymer injection site was collected, with local distribution of SQP33 protodrug and active Dox shown in (C) and (D). All samples were analyzed by LC-MS for both analytes and are displayed as mean + SEM.

Synthetic Procedures:

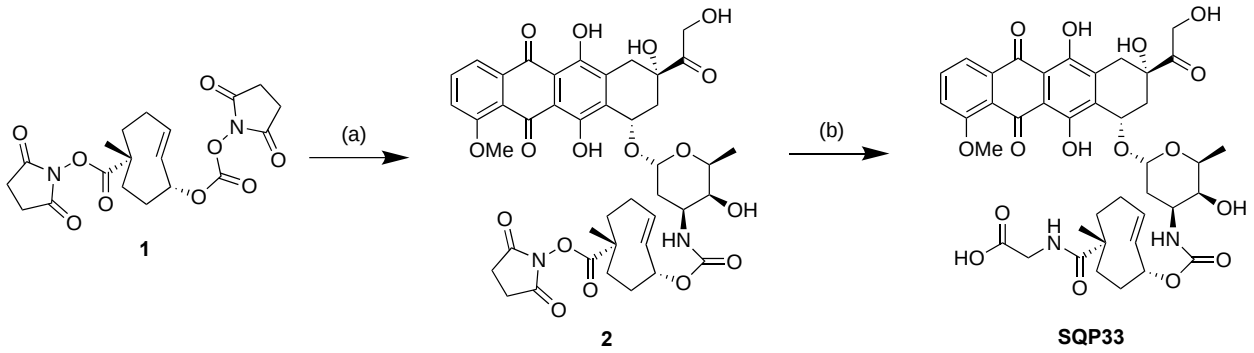

Synthesis of the compound 2

Compound **1** was synthesized using previously reported method [*Bioconj. Chem.* **2016**, *27*, 1697-1706]. Compound **1** (1.75 g, 4.14, 1.2 equiv) was added in one portion to DMF (75 mL) solution of Dox·HCl (2 g, 3.45 mmol) and DIPEA (1.34 g, 10.35 mmol, 3 equiv). The resulting solution was stirred for 12 h and quenched with water (150 mL). The product was extracted with EtOAc (3x200 mL) and the combined organic phases were washed with brine and dried over Na_2SO_4. After removal of the organic solvents, the residue was purified by flash chromatography using a gradient of MeOH in CH_2Cl_2 (0-5%) to afford compound **2**. Yield = 2.16 g, 73%. The NMR spectrum is identical to the previously published spectra [*Bioconj. Chem.* **2016**, *27*, 1697-1706].

Synthesis of SQP33

TMS-Cl (638 mg, 5.9 mmol, 10 equiv) was added in one portion to a suspension of glycine (440 mg, 5.9 mmol, 10 equiv) in 50 mL of $CHCl_3$-MeCN (60%-40%). The resulting mixture was stirred at reflux (80 ^oC) for 2 h and then cooled to rt. DIPEA (2 mL, 12 mmol, 20 equiv) and Dox-TCO-NHS **2** (500 mg, 0.58 mmol) were added at room temperature and the mixture was then stirred at 65 ^oC for 6 h. After removal of the solvents, the residue was dissolved in water (5 mL) and purified by HPLC using a 0-50% gradient of MeCN (0.1% formic acid) in water (0.1% formic acid) to afford SQP33 (235 mg, 49%) as orange solid.

^{1}H NMR (500 MHz, DMSO) δ 13.93 (s, 1H), 13.17 (s, 1H), 7.77 (dd, *J* = 42.5, 36.0 Hz, 2H), 7.56 (s, 2H), 6.72 – 6.56 (m, 1H), 5.94 – 5.72 (m, 1H), 5.65 – 5.51 (m, 1H), 5.40 (s, 1H), 5.21 (s, 1H), 4.96 – 4.82 (m, 2H), 4.59 (s, 2H), 4.17 (d, *J* = 6.5 Hz, 1H), 3.94 (s, 3H), 3.79 – 3.52 (m, 4H), 3.52 – 3.36 (m, 2H), 3.06 – 2.88 (m, 1H), 2.88 – 2.73 (m, 1H), 2.28 – 1.94 (m, 5H), 1.91 – 1.77 (m, 3H), 1.77 – 1.56 (m, 3H), 1.48 (t, *J* = 11.5 Hz, 2H), 1.12 (t, *J* = 21.0 Hz, 3H), 0.97 (s, 3H).
^{13}C NMR (125 MHz, DMSO) δ 213.32, 186.11, 185.81, 182.18, 172.19, 160.73, 155.92, 155.75, 154.52, 135.64, 134.52, 134.06, 133.56, 131.26, 131.10, 119.66, 118.97, 118.64, 110.74, 110.51, 100.87, 75.93, 72.20, 69.73, 68.84, 68.68, 67.25, 64.36, 55.62, 45.01, 43.96, 40.93, 38.97, 35.72, 35.39, 32.55, 30.66, 30.46, 29.46, 16.80, 15.93, 15.78.
HRMS (*ESI*) *m/z*: calcd. for $C_{40}H_{46}N_2O_{16}$ $[M+Na]^+$ 833.2740, found 833.2743.

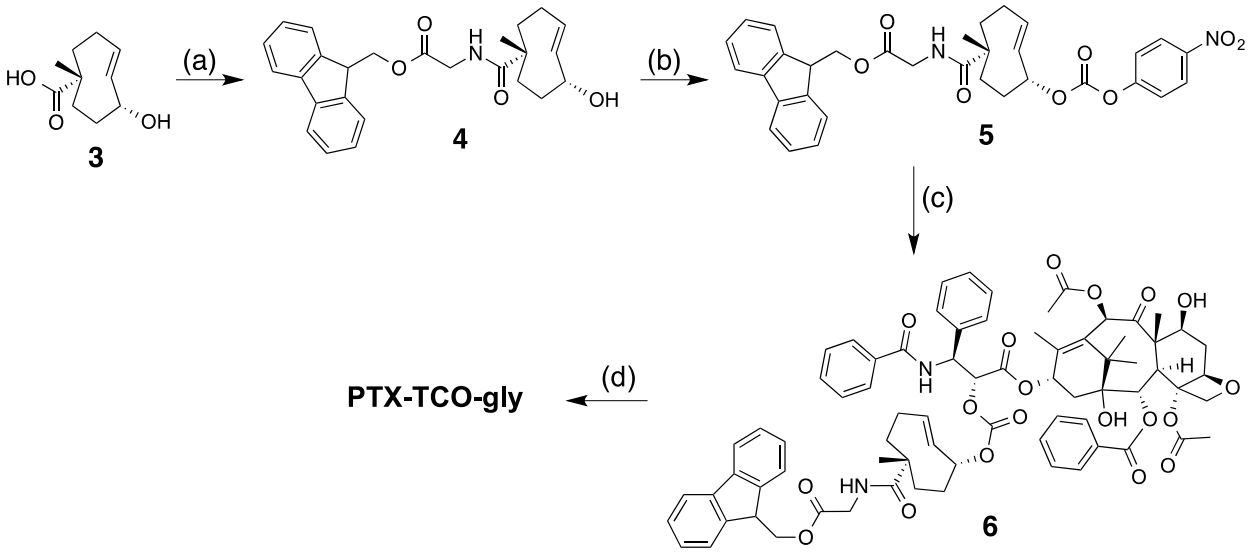

Synthesis of the compound 4

Compound **3** (1.0 g, 5.4 mmol) and Fmoc-protected glycine·HCl (3.15 g, 10.8 mmol) were dissolved in anhydrous DMF (25 mL). HATU (4.13 g, 10.8 mmol mmol) and DIPEA (3.5 g, 27.1 mmol) were added and the resulting mixture was stirred overnight. The reaction mixture was poured onto water (50 mL). The product was extracted with EtOAc (3 x 30 mL). The combined organic phase was dried with Na_2SO_4 and concentrated. The residue was purified by flash chromatography using a gradient of EtOAc in hexanes (20-40%) to give compound **4** (2.0 g, 87%).

^{1}H NMR (500 MHz, $CDCl_3$) δ 7.76 (d, *J* = 7.6 Hz, 2H), 7.57 (d, *J* = 7.5 Hz, 2H), 7.40 (t, *J* = 7.5 Hz, 2H), 7.36 – 7.24 (m, 2H), 6.26 (t, *J* = 4.8 Hz, 1H), 6.14 – 6.00 (m, 1H), 5.62 (d, *J* = 16.6 Hz, 1H), 4.44 (d, *J* = 7.1 Hz, 3H), 4.21 (t, *J* = 7.0 Hz, 1H), 4.06 (t, *J* = 12.1 Hz, 2H), 2.79 (t, *J* = 5.2 Hz, 3H), 2.64 (d, *J* = 14.7 Hz, 1H), 2.36 – 2.16 (m, 2H), 2.15 – 1.96 (m, 2H), 1.85 (ddd, *J* = 32.9, 21.9, 10.1 Hz, 3H), 1.58 (dd, *J* = 15.6, 6.2 Hz, 1H), 1.13 (d, *J* = 21.4 Hz, 3H).
^{13}C NMR (126 MHz, $CDCl_3$) δ 181.01, 170.31, 143.44, 143.42, 141.27, 135.17, 130.11, 127.92, 127.22, 125.02, 120.10, 69.51, 67.14, 46.62, 45.76, 44.38, 41.63, 38.63, 38.40, 31.03, 30.10, 17.69.
HRMS (*ESI*) *m/z*: calcd. for $C_{26}H_{29}NO$ $[M+H]^+$ 420.2169, found 420.2166.

Synthesis of the compound 5

Pyridine (1.13 mg, 14.3 mmol) was added to a solution of **8** (2.0 g, 4.77 mmol) in freshly distilled CH_2Cl_2 (20 mL). A solution of p-nitrophenyl chloroformate (1.24 g, 6.2 mmol) in CH_2Cl_2 (5 mL) was slowly added via syringe at 0 °C. The mixture was stirred at rt for 12 h. The solvent was removed under reduced pressure. The product was purified by flash chromatography using a gradient of EtOAc in hexanes (20-40%) to give compound **5** (1.65 g, 60%).

^{1}H NMR (500 MHz, $CDCl_3$) δ 8.32 – 8.26 (m, 2H), 7.79 (d, *J* = 7.5 Hz, 2H), 7.59 (d, *J* = 7.5 Hz, 2H), 7.47 – 7.38 (m, 4H), 7.34 (td, *J* = 7.5, 0.9 Hz, 2H), 6.13 – 5.98 (m, 2H), 5.67 (dd, *J* = 16.7, 2.3 Hz, 1H), 5.31 (s, 1H), 4.50 (d, *J* = 7.1 Hz, 2H), 4.25 (t, *J* = 7.0 Hz, 1H), 4.20 – 4.03 (m, 2H), 2.46 – 2.38 (m, 1H), 2.38 – 2.26 (m, 1H), 2.18 (tdd, *J* = 27.2, 17.0, 10.1 Hz, 2H), 2.07 – 1.85 (m, 3H), 1.77 (dd, *J* = 15.3, 6.3 Hz, 2H), 1.22 (d, *J* = 28.2 Hz, 3H).
^{13}C NMR (126 MHz, $CDCl_3$) δ 180.09, 170.17, 155.55, 151.58, 145.37, 143.35, 141.31, 132.87, 129.43, 127.98, 127.24, 125.33, 124.97, 121.79, 120.15, 67.24, 46.63, 45.50, 44.33, 41.63, 35.75, 31.16, 31.04, 17.86.
HRMS (*ESI*) *m/z*: calcd. for $C_{33}H_{32}N_2O_8$ $[M+H]^+$ 585.2231, found 585.2237.

Synthesis of PTX-TCO-gly

Compound **9** (47.2 mg, 0.082 mmol) and DMAP (14 mg, 0.117 mmol) were added to a solution of PTX (50.0 mg, 0.058 mmol) in CH_2Cl_2 (10 mL). The resulting solution was stirred for 3 d. The reaction was quenched with water (30 mL). The product was extracted with CH_2Cl_2 (3 x 50 mL) and the combined organic phase was dried with Na_2SO_4 and concentrated to give crude compound **6** which was used without further purification. Compound **6** was added to a solution of 10% piperidine in DMF (8 mL). The resulting mixture was stirred overnight at rt. The reaction was quenched with water (20 mL) and the product was extracted with EtOAc (3 x 30 mL). The combined organic phase was washed with water (3 x 50 mL) and brine, and concentrated under reduced pressure. The residue was purified by flash chromatography using a gradient of MeOH in CH_2Cl_2 (5-10%) to give **PTX-TCO-gly** (20 mg, 30% over 2 steps).

^{1}H NMR (500 MHz, MeOD) δ 8.13 (d, *J* = 8.3 Hz, 2H), 7.85 (d, *J* = 8.3 Hz, 2H), 7.69 (t, *J* = 7.0 Hz, 1H), 7.60 (td, *J* = 7.7, 3.0 Hz, 2H), 7.58 – 7.51 (m, 3H), 7.47 (t, *J* = 7.6 Hz, 4H), 7.29 (dd, *J* = 16.0, 7.5 Hz, 1H), 6.46 (d, *J* = 3.6 Hz, 1H), 6.09 (dd, *J* = 16.2, 8.0 Hz, 1H), 6.04 – 5.79 (m, 2H), 5.73 – 5.61 (m, 2H), 5.52 (dd, *J* = 16.8, 6.8 Hz, 1H), 5.17 (d, *J* = 15.5 Hz, 1H), 5.01 (d, *J* = 9.6 Hz, 1H), 4.39 – 4.31 (m, 1H), 4.20 (s, 2H), 3.82 (dd, *J* = 7.0, 4.3 Hz, 2H), 2.56 – 2.45 (m, 1H), 2.43 (d, *J* = 1.7 Hz, 3H), 2.33 – 2.11 (m, 7H), 2.11 – 1.88 (m, 7H), 1.88 – 1.73 (m, 3H), 1.67 (d, *J* = 2.3 Hz, 4H), 1.15 (s, 8H).

^{13}C NMR (126 MHz, MeOD) δ 203.77, 170.29, 169.96, 168.99, 168.83, 166.27, 153.62, 153.55, 140.94, 140.79, 136.74, 134.02, 133.58, 133.48, 133.25, 131.99, 131.73, 131.58, 129.99, 129.81, 128.73, 128.35, 128.20, 127.28, 84.51, 80.84, 77.62, 77.04, 76.96, 76.77, 76.62, 76.07, 75.40, 74.85, 71.76, 70.91, 57.82, 54.14, 54.05, 46.47, 45.04, 44.00, 43.19, 36.11, 35.26, 35.11, 34.99, 30.59, 30.51, 29.35, 25.57, 21.89, 21.01, 19.43, 16.83, 13.57, 9.08.

HRMS (*ESI*) *m/z*: calcd for $C_{60}H_{68}N_2O_{19}$ $[M+H]^+$ 1121.4489, found 1121.4495.

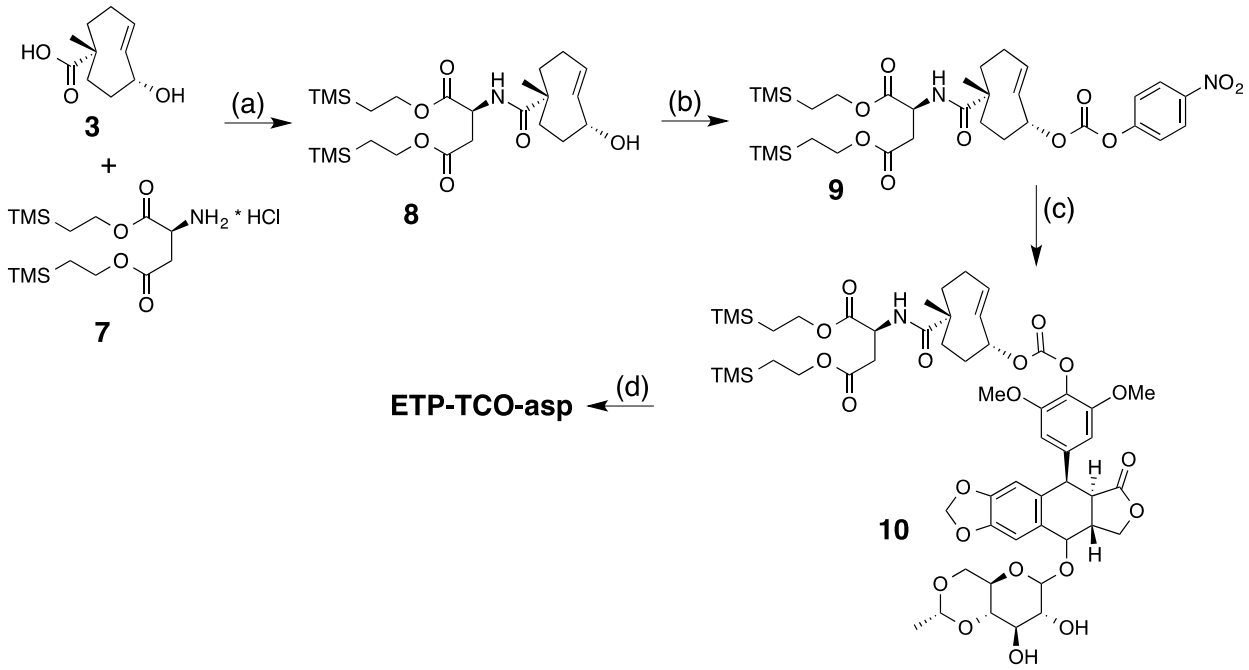

Synthesis of the compound 8
Compound **3** (300 mg, 1.63 mmol) and TMS ethyl aspartate **4** (1.21 g, 3.26 mmol) were dissolved in anhydrous DMF (15 mL). HATU (1.24 g, 3.26 mmol) and DIPEA (1.05 g, 8.56 mmol) were added and the resulting mixture was stirred overnight. The reaction mixture was poured onto water (50 mL). The product was extracted with EtOAc (3 x 30 mL). The combined organic phase was dried with Na_2SO_4 and concentrated. The residue was purified by flash chromatography using a gradient of EtOAc in hexanes (20-40%) to give compound **8** (700 mg, 86%).

^{1}H NMR (500 MHz, $CDCl_3$) δ 6.57 (dd, *J* = 7.9, 2.9 Hz, 1H), 6.10 – 6.00 (m, 1H), 5.63 (dd, *J* = 16.6, 2.4 Hz, 1H), 4.73 (qd, *J* = 8.4, 4.3 Hz, 1H), 4.45 (d, *J* = 4.8 Hz, 1H), 4.26 – 4.18 (m, 2H), 4.18 – 4.13 (m, 2H), 2.94 (dq, *J* = 16.2, 4.1 Hz, 1H), 2.75 (dt, *J* = 16.9, 4.8 Hz, 1H), 2.26 (dqd, *J* = 35.4, 11.9, 3.7 Hz, 2H), 2.14 – 2.04 (m, 2H), 1.98 (ddd, *J* = 19.3, 9.7, 5.9 Hz, 1H), 1.93 – 1.85 (m, 1H), 1.85 – 1.76 (m, 2H), 1.56 (ddd, *J* = 28.0, 15.5, 6.2 Hz, 1H), 1.10 (s, 3H), 1.00 – 0.95 (m, 4H), 0.04 – 0.01 (m, 18H).
^{13}C NMR (126 MHz, $CDCl_3$) δ 180.20, 171.34, 171.12, 135.12, 130.12, 69.47, 64.17, 63.28, 48.65, 45.82, 44.32, 38.38, 36.15, 30.96, 29.88, 17.60, 17.33, 17.29, -1.55, -1.56.
HRMS (*ESI*) *m/z*: calcd for $C_{24}H_{45}NO_6Si_2$ $[M+H]^+$ 500.2858, found 500.2856.

Synthesis of compound 9
Pyridine (332 mg, 4.2 mmol) was added to a solution of compound **8** (700 mg, 1.4 mmol) in freshly distilled CH_2Cl_2 (20 mL). A solution of p-nitrophenyl chloroformate (366 mg, 1.8 mmol) in DCM (5 mL) was slowly added via syringe at 0 °C. The mixture was stirred at rt for 12 h. The solvent was removed under reduced pressure. The product was purified by flash chromatography using a gradient of EtOAc in hexanes (0-20%) to give compound **9** (440 mg, 47%).

^{1}H NMR (500 MHz, $CDCl_3$) δ 8.33 – 8.22 (m, 2H), 7.45 – 7.37 (m, 2H), 6.63 (d, *J* = 7.8 Hz, 1H), 6.14 – 6.03 (m, 1H), 5.67 (dd, *J* = 16.7, 2.5 Hz, 1H), 5.30 (s, 1H), 4.79 – 4.69 (m, 1H), 4.32 – 4.14 (m, 4H), 2.99 (dd, *J* = 17.0, 4.4 Hz, 1H), 2.79 (dd, *J* = 17.0, 4.5 Hz, 1H), 2.43 – 2.15 (m, 4H), 2.06 – 1.86 (m, 3H), 1.24 – 1.10 (m, 4H), 1.05 – 0.94 (m, 4H), 0.09 – 0.01 (m, 18H).
^{13}C NMR (125 MHz, $CDCl_3$) δ 179.54, 171.42, 171.09, 155.56, 151.56, 145.38, 132.91, 129.38, 125.30, 121.75, 64.32, 63.40, 48.70, 45.48, 44.33, 36.13, 35.75, 31.11, 30.94, 17.83, 17.37, -1.54.
HRMS (*ESI*) *m/z*: calcd for $C_{31}H_{48}N_2O_{10}Si_2$ $[M+H]^+$ 665.2920, found 665.2919.

Synthesis of ETP-TCO-asp
Compound **9** (1.17 g, 1.77 mmol) and Cs_2CO_3 (1.3 g, 4.1 mmol) were added to a solution of ETP (800 mg, 1.36 mmol) in DMF (10 mL). The resulting solution was stirred for 3 d. The reaction was quenched with water (30 mL). The product was extracted with EtOAc (3 x 50 mL) and the combined organic phase was dried with Na_2SO_4 and concentrated. The residue was purified by flash chromatography using a gradient of EtOAc in hexanes (20-50%) to give compound **10** (210 mg, 49%).
1M TBAF solution in THF (2 mL) was added to a solution of compound **10** (400 mg, 0.36 mmol) in anhydrous THF (8 mL). The resulting mixture was stirred overnight at rt. The reaction was quenched with water (20 mL) and the product was extracted with EtOAc (3 x 30 mL). The combined organic phase was washed with water (6 x 50 mL, to get rid of excess TBAF) and brine, and concentrated under reduced pressure. The residue was recrystallized from EtOAc/Hexane to give **ETP-TCO-asp** (212 mg, 66%).

^{1}H NMR (500 MHz, MeOD) δ 7.15 (d, *J* = 3.9 Hz, 1H), 6.66 – 6.60 (m, 2H), 6.52 (d, *J* = 6.0 Hz, 1H), 6.03 – 5.92 (m, 3H), 5.71 (dd, *J* = 16.7, 2.4 Hz, 1H), 5.19 (s, 1H), 4.76 (q, *J* = 5.0 Hz, 1H), 4.67 (dd, *J* = 13.5, 6.7 Hz, 1H), 4.52 – 4.38 (m, 3H), 4.30 (d, *J* = 7.8 Hz, 1H), 4.12 (dd, *J* = 10.3, 4.3 Hz, 1H), 3.67 (dd, *J* = 10.6, 5.1 Hz, 1H), 3.60 – 3.41 (m, 3H), 3.31 – 3.17 (m, 5H), 2.93 – 2.76 (m, 2H), 2.41 – 2.26 (m, 2H), 2.18 (ddd, *J* = 25.2, 16.8, 6.0 Hz, 2H), 1.97 (dd, *J* = 17.5, 6.5 Hz, 2H), 1.84 (d, *J* = 13.3 Hz, 1H), 1.69 (dt, *J* = 20.7, 10.9 Hz, 2H), 1.51 – 1.30 (m, 4H), 1.37 – 1.24 (m, 4H), 1.17 (d, *J* = 13.1 Hz, 3H). ^{13}C NMR (125 MHz, MeOD) δ 182.62, 181.74, 174.57, 153.76, 153.66, 149.30, 148.16, 142.30, 133.37, 133.22, 131.23, 130.06, 129.38, 110.21, 108.88, 106.40, 102.98, 102.61, 100.72, 89.04, 81.63, 77.92, 76.45, 75.92, 74.80, 70.14, 69.21, 67.52, 64.92, 56.81, 55.43, 54.89, 50.58, 46.52, 46.43, 45.49, 45.02, 40.70, 36.78, 36.60, 32.01, 31.91, 20.63, 18.19.
HRMS (*ESI*) *m/z*: calcd for $C_{44}H_{52}NO_{20}$ $[M + H]^+$ 914.3077, found 914.3078.

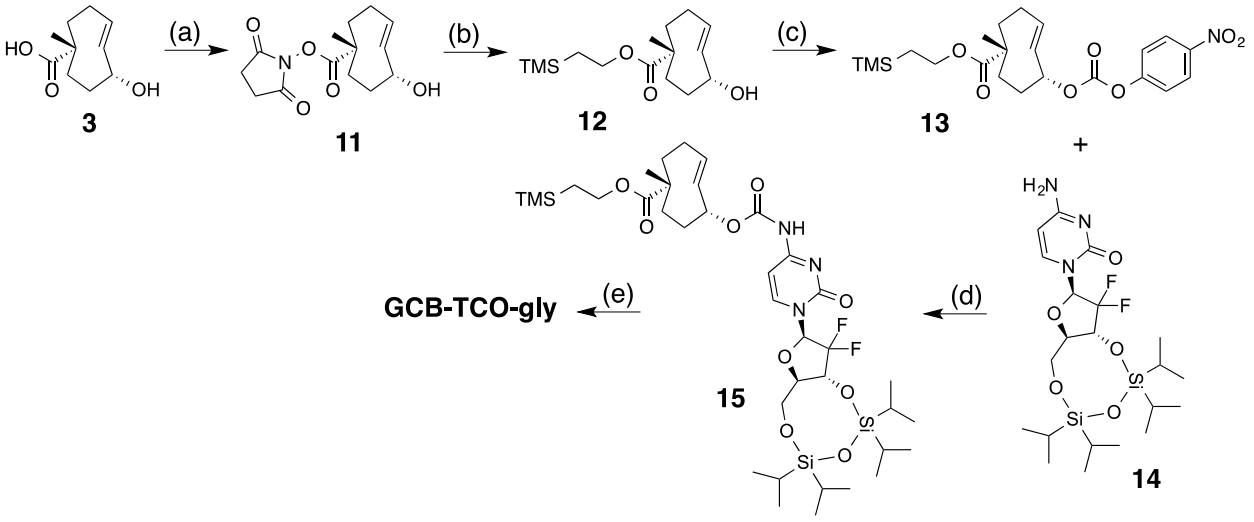

Synthesis of compound 11
DSC (1.6 g, 6.5 mmol) was added in one portion to a stirring solution of compound **3** (1.2 g, 6.5 mmol) and DIPEA (2.5 g, 19.5 mmol) in CH_3CN (50 mL). The resulting solution was allowed to stir for 12 h at rt. After evaporation of solvents under reduced pressure, the residue was purified by flash chromatography to give compound **11** (800 mg, 48%).

^{1}H NMR (500 MHz, $CDCl_3$) δ 6.10 – 5.92 (m, 1H), 5.60 (dd, *J* = 16.6, 2.0 Hz, 1H), 4.43 (s, 1H), 2.77 (d, *J* = 3.3 Hz, 5H), 2.46 (s, 1H), 2.41 – 2.30 (m, 1H), 2.30 – 2.17 (m, 2H), 2.15 – 1.99 (m, 2H), 1.99 – 1.91 (m, 1H), 1.88 – 1.77 (m, 2H), 1.25 (s, 3H).
^{13}C NMR (126 MHz, $CDCl_3$) δ 174.67, 169.65, 135.33, 129.88, 69.30, 44.45, 44.36, 38.30, 30.49, 29.29, 25.63, 17.76.
HRMS (*ESI*) *m/z*: calcd for $C_{14}H_{19}NO_5$ $[M+H]^+$ 282.1136, found 282.1135.

Synthesis of compound 12
NaH (994 mg, 24.9 mmol) was added in three portions to a solution of TMS ethanol (1.47 g, 12.4 mmol) in anhydrous THF (50 mL) at 0 °C. The mixture was stirred at 0 °C for 30 min and a solution of **11** (700 mg, 2.49 mmol) in anhydrous THF (15 mL) was added slowly via syringe. The reaction was warmed to rt and the stirring was continued for 5 h. The reaction mixture was poured into ice water and extracted with EtOAc (3×50 mL). The combined extracts were washed with sat. NH_4Cl_{aq} and dried over Na_2SO_4. After concentration, the residue was purified by flash chromatography using a gradient of EtOAc in hexanes (0-25%) to give compound **12** (570 mg, 70%).

^{1}H NMR (400 MHz, CDCl3) δ 6.15 – 5.94 (m, 1H), 5.64 (dd, J = 16.6, 2.0 Hz, 1H), 4.48 (s, 1H), 4.19 – 4.01 (m, 2H), 2.36 – 2.10 (m, 3H), 1.87 (dd, J = 24.9, 11.3 Hz, 3H), 1.61 – 1.48 (m, 3H), 1.10 (s, 3H), 0.98 (d, J = 8.4 Hz, 2H), 0.04 (s, 9H).
^{13}C NMR (100 MHz, $CDCl_3$) δ 179.99, 134.93, 130.42, 69.66, 62.73, 44.87, 44.35, 38.19, 30.84, 29.63, 18.12, 17.26, -1.49.
HRMS (*ESI*) *m/z*: calcd for $C_{15}H_{28}O_3Si$ $[M+H]^+$ 285.1880, found 285.1885.

Synthesis of compound 13
Pyridine (750 mg, 9.5 mmol) was added to a solution of compound **12** (900 mg, 3.16 mmol) in freshly distilled CH_2Cl_2 (20 mL). The resulting mixture was cooled to 0 ^{o}C and a solution of p-nitrophenyl chloroformate (956 mg, 4.7 mmol) in CH_2Cl_2 (5 mL) was slowly added via syringe. The mixture was stirred at rt for 12 h. The solvents were removed under reduced pressure and the resulting residue was purified by flash chromatography using a gradient of EtOAc in hexanes (0-10%) to give compound **13** (900 mg, 64%).
^{1}H NMR (400 MHz, CDCl3) δ 8.28 (d, J = 9.1 Hz, 2H), 7.40 (d, J = 9.1 Hz, 2H), 6.13 – 5.96 (m, 1H), 5.64 (d, J = 16.7 Hz, 1H), 5.29 (s, 1H), 4.12 (dd, J = 11.2, 6.0 Hz, 2H), 2.42 – 2.12 (m, 4H), 2.04 – 1.83 (m, 3H), 1.79 – 1.68 (m, 1H), 1.14 (s, 3H), 1.04 – 0.93 (m, 2H), 0.05 (s, 9H).
^{13}C NMR (126 MHz, $CDCl_3$) δ 179.37, 155.57, 151.56, 145.36, 133.10, 129.34, 125.27, 121.76, 62.92, 44.78, 44.38, 35.63, 30.95, 30.57, 18.33, 17.34, -1.51.
HRMS (*ESI*) *m/z*: calcd for $C_{22}H_{31}NO_7Si$ $[M+H]^+$ 450.1943, found 450.1949.

Synthesis of compound 14
1,3-Dichloro-1,1,3,3-tetraisopropyldisiloxane (3.47 g, 11.0 mmol) was added to a solution of GCB (3 g, 10.0 mmol) in pyridine (25 mL) and the mixture was stirred at rt overnight. After removal of the solvent, the residue was purified by flash chromatography using a gradient of MeOH in CH_2Cl_2 (0-10%) to give compound **14** (3.9 g, 77%).

^{1}H NMR (400 MHz, CDCl3) δ 8.75 – 8.26 (m, 1H), 7.58 (t, J = 8.3 Hz, 1H), 6.16 (t, J = 9.5 Hz, 2H), 4.37 – 4.11 (m, 2H), 4.02 (d, J = 13.4 Hz, 1H), 3.92 (d, J = 9.2 Hz, 1H), 1.04 (dd, J = 22.1, 17.2 Hz, 28H).
^{13}C NMR (100 MHz, $CDCl_3$) δ 165.70, 155.37, 139.67, 123.52, 121.46, 119.40, 95.52, 84.71, 84.48, 84.20, 79.14, 69.34, 69.16, 68.99, 59.65, 17.37, 17.27, 17.23, 17.20, 16.91, 16.79, 16.64, 13.39, 12.89, 12.73, 12.38.
HRMS (*ESI*) *m/z*: calcd for $C_{21}H_{37}F_2N_3O_5Si_2$ $[M+H]^+$ 506.2313, found 506.2315.

Synthesis of the compound 15
NaH (65 mg, 1.6 mmol) was added in three portions to a solution of compound **14** (330 mg, 0.65 mmol) in DMF (15 mL) at 0 ^{o}C. The mixture was allowed to stir for 30 min at 0 ^{o}C. A solution of **13** (350 mg, 0.78 mmol) in DMF (3 mL) was added via syringe under at 0 ^{o}C. The reaction was slowly warmed up to rt and stirred for 12 h. The reaction was quenched with water (20 mL). The product was extracted with EtOAc (3x30 mL) and the combined organic phase was dried Na_2SO_4 and concentrated. The residue was purified by flash chromatography using a gradient of EtOAc in hexanes (10-50%) to give compound **15** (300 mg, 56%).

^{1}H NMR (400 MHz, CDCl3) δ 8.15 (d, J = 5.0 Hz, 1H), 7.34 – 7.21 (m, 1H), 6.34 (s, 1H), 6.06 – 5.88 (m, 1H), 5.61 (d, J = 16.8 Hz, 1H), 5.25 (s, 1H), 4.44 (dd, J = 21.6, 12.4 Hz, 1H), 4.16 – 4.05 (m, 4H), 2.19 (ddd, J = 45.1, 35.6, 16.7 Hz, 4H), 1.97 – 1.79 (m, 3H), 1.71 – 1.56 (m, 1H), 1.08 (dd, J = 16.8, 9.7 Hz, 30H), 0.98 – 0.91 (m, 3H), 0.04 (d, J = 11.2 Hz, 9H).
^{13}C NMR (126 MHz, $CDCl_3$) δ 179.79, 163.26, 155.27, 151.78, 143.96, 132.67, 129.84, 124.35, 122.27, 120.21, 95.78, 85.06, 84.84, 84.55, 81.10, 74.02, 68.31, 68.12, 67.95, 62.98, 59.44, 44.63, 44.35, 35.60, 31.88, 30.93, 30.58, 22.69, 18.19, 17.39, 17.29, 17.25, 17.19, 14.11, 13.47, 13.38, 13.10, 12.87, -1.52.
HRMS (*ESI*) *m/z*: calcd for $C_{37}H_{63}F_2N_3O_9Si_3$ $[M+H]^+$ 816.3913, found 816.3916.

Synthesis of GCB-TCO-acid
Stirred compound **15** (300 mg, 0.56 mmol) in 1M THF solution of TBAF (3 mL) for 18 h. The reaction was quenched with water (20 mL) and extracted with EtOAc (3 x 30 mL). The combined organic phase was washed with water and brine, and concentrated. The residue was recrystallized in EtOAc/Hexane to give **GCB-TCO-acid** (120 mg, 68%).
^{1}H NMR (400 MHz, MeOD) δ 8.31 (d, J = 7.7 Hz, 1H), 7.32 (d, J = 7.6 Hz, 1H), 6.31 – 6.21 (m, 1H), 6.08 – 5.92 (m, 1H), 5.69 (d, J = 16.7 Hz, 1H), 5.27 (s, 1H), 4.31 (dd, J = 20.7, 12.1 Hz, 1H), 4.04 – 3.90 (m, 2H), 3.81 (dd, J = 12.3, 2.5 Hz, 1H), 2.31 – 2.15 (m, 3H), 2.15 – 1.95 (m, 3H), 1.89 (d, J = 13.4 Hz, 1H), 1.13 (s, 3H);
^{13}C NMR (125 MHz, MeOD) δ 182.56, 164.08, 156.06, 152.33, 144.25, 132.00, 130.26, 130.21, 124.58, 123.09, 122.52, 121.28, 120.46, 117.59, 95.67, 84.77, 81.43, 73.81, 68.88, 68.69, 58.94, 44.80, 44.28, 35.16, 30.57, 30.38, 17.56
ESI HRMS calcd for $C_{20}H_{25}F_2N_3O_8$ $[M + H]^+$ 474.1682, found 474.1681.

SQL70 **Synthesis**

Synthesis of SQL70 follows an optimized 3-step process that includes: (i) condensing the sodium salt of HA with a tetrazine derivative (3-methyl-1,2,4,5-tetrazine-6-phenylmethanamine HCl) in the presence of excess carbodiimide activating agent, (ii) purification using tangential flow filtration (TFF) to remove low molecular weight reagents and by-products, and (iii) sterilization by ultrafiltration. The derivatization reaction occurs in N-morpholinoethanesulfonic acid (MES) buffered aqueous solvent with activation of the HA carboxylic acid group by N-hydroxysulfosuccinimide and N,N-(dimethylaminopropyl)-N-ethyl carbodiimide HCl. The resulting product is conjugated with tetrazine at 19 weight%.

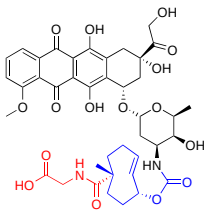

SQP33

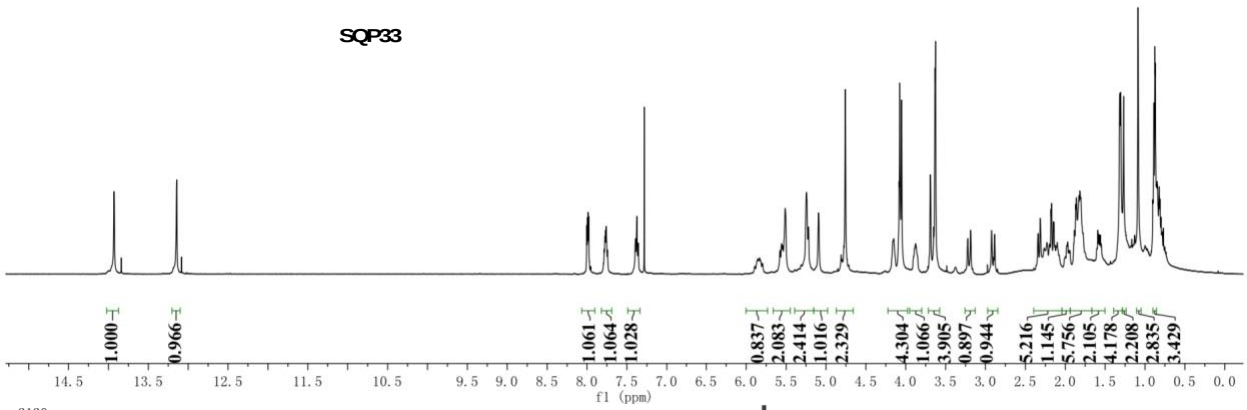
1.000
0.966
1.061
1.064
1.028
0.837
2.083
2.414
1.016
2.329
4.304
1.066
3.905
0.897
0.944
5.216
1.145
5.756
2.105
4.178
2.208
2.835
3.429
f1 (ppm)

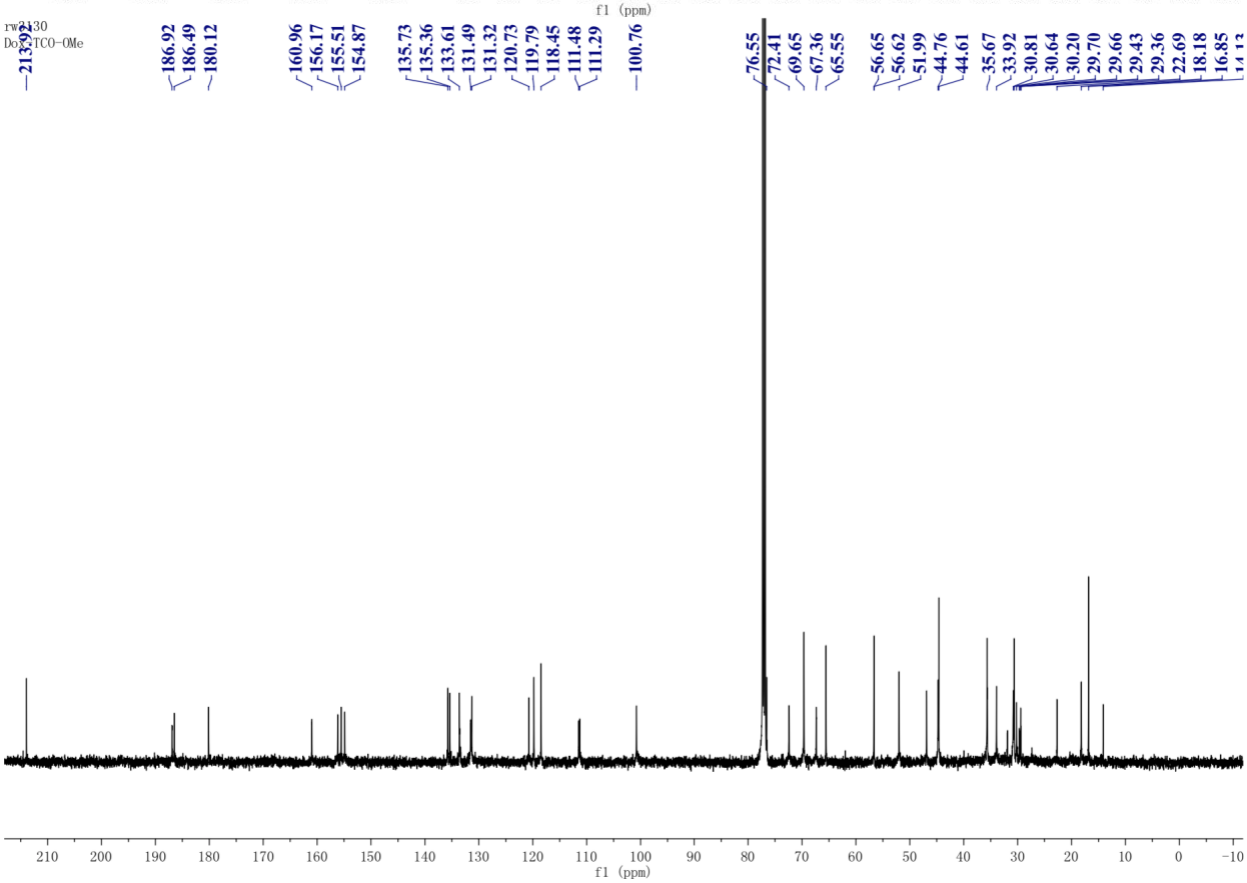
rw2130
DoESTCO-OMe
213.92
186.92
186.49
180.12
160.96
156.17
155.51
154.87
135.73
135.36
133.61
131.49
131.32
120.73
119.79
118.45
111.48
111.29
100.76
76.55
72.41
69.65
67.36
65.55
56.65
56.62
51.99
44.76
44.61
35.67
33.92
30.81
30.64
30.20
29.70
29.66
29.43
29.36
22.69
18.18
16.85
f1 (ppm)

rw3164

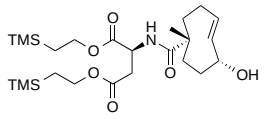

8

rw3164

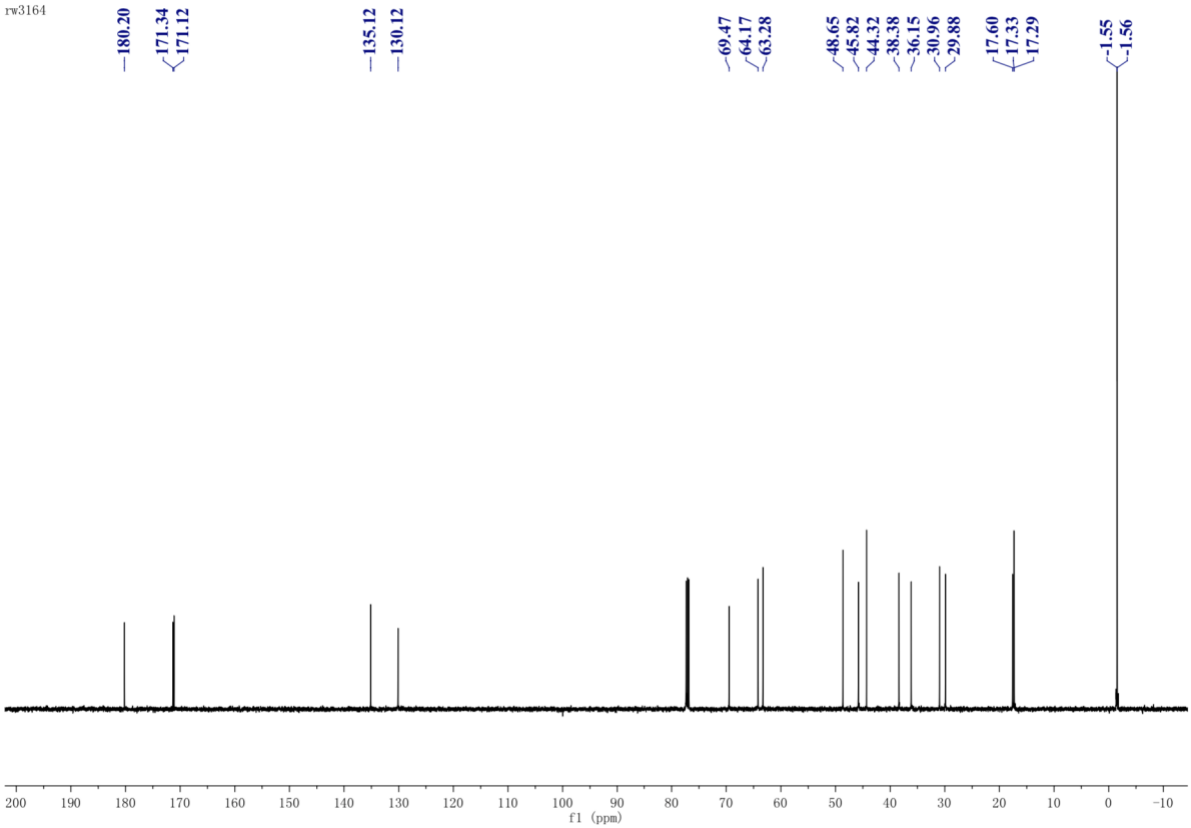

rw3011
1H rw3011

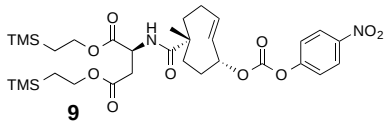

9

rw3011
13C rw3011

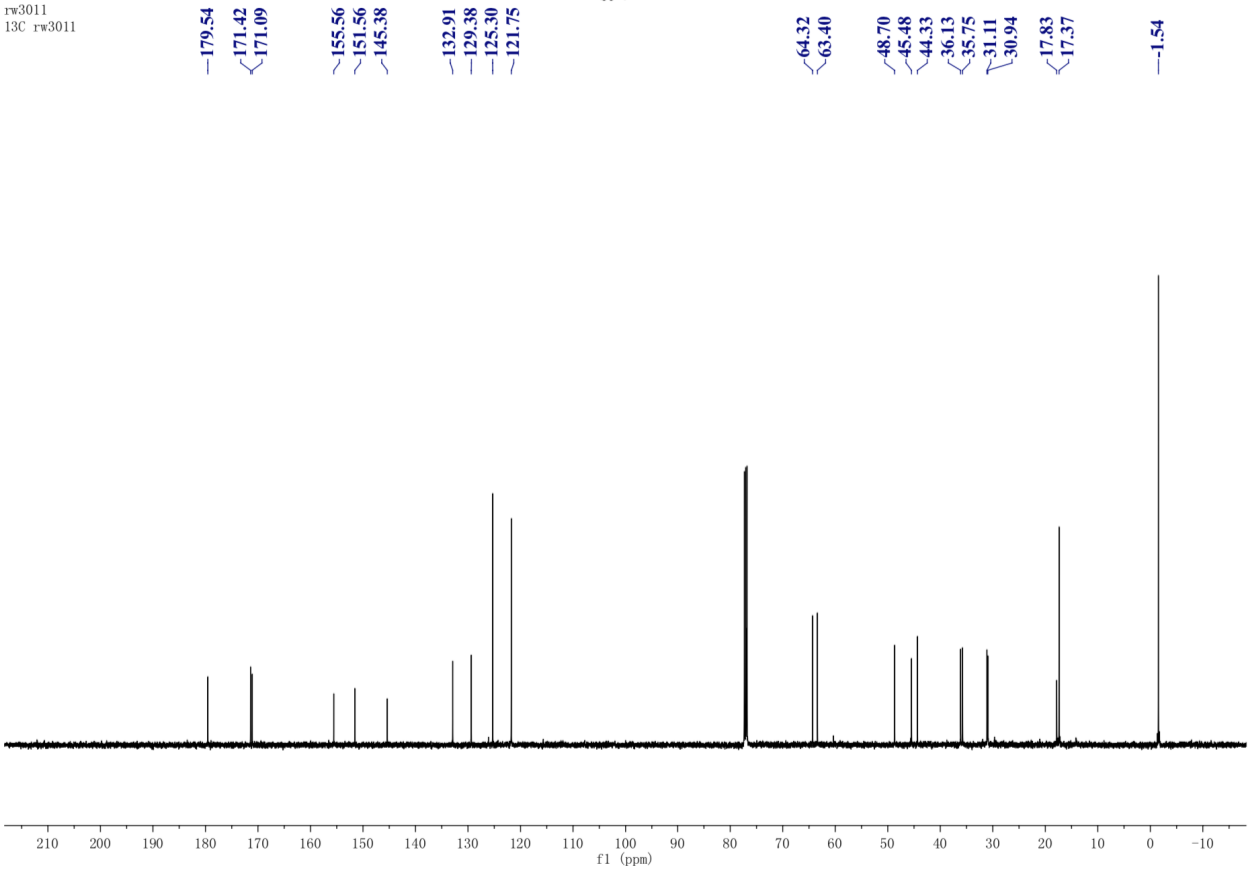

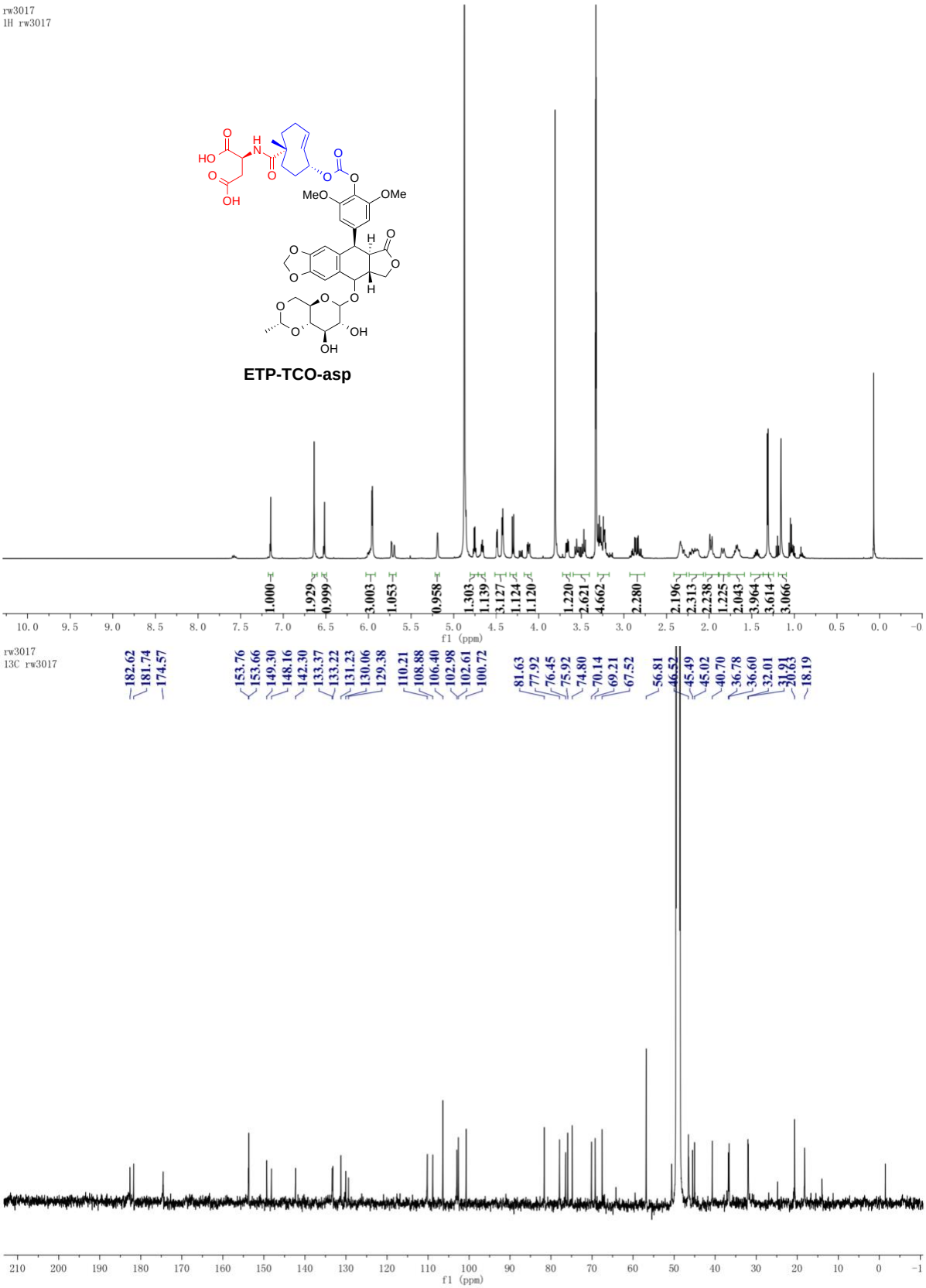
rw3017
1H rw3017
ETP-TCO-asp
1.000
1.929
0.999
3.003
1.053
0.958
1.303
1.139
3.127
1.124
1.120
1.220
2.621
4.662
2.280
2.196
2.313
2.238
1.225
2.043
3.964
3.614
3.066
f1 (ppm)
rw3017
13C rw3017
182.62
181.74
174.57
153.76
153.66
149.30
148.16
142.30
133.37
133.22
131.23
130.06
129.38
110.21
108.88
106.40
102.98
102.61
100.72
81.63
77.92
76.45
75.92
74.80
70.14
69.21
67.52
56.81
46.52
45.49
45.02
40.70
36.78
36.60
32.01
31.91
30.63
18.19
f1 (ppm)

rw3055
1H rw3055

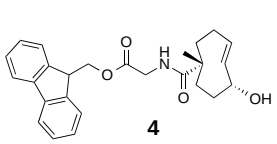

4

rw3055
1H rw3055

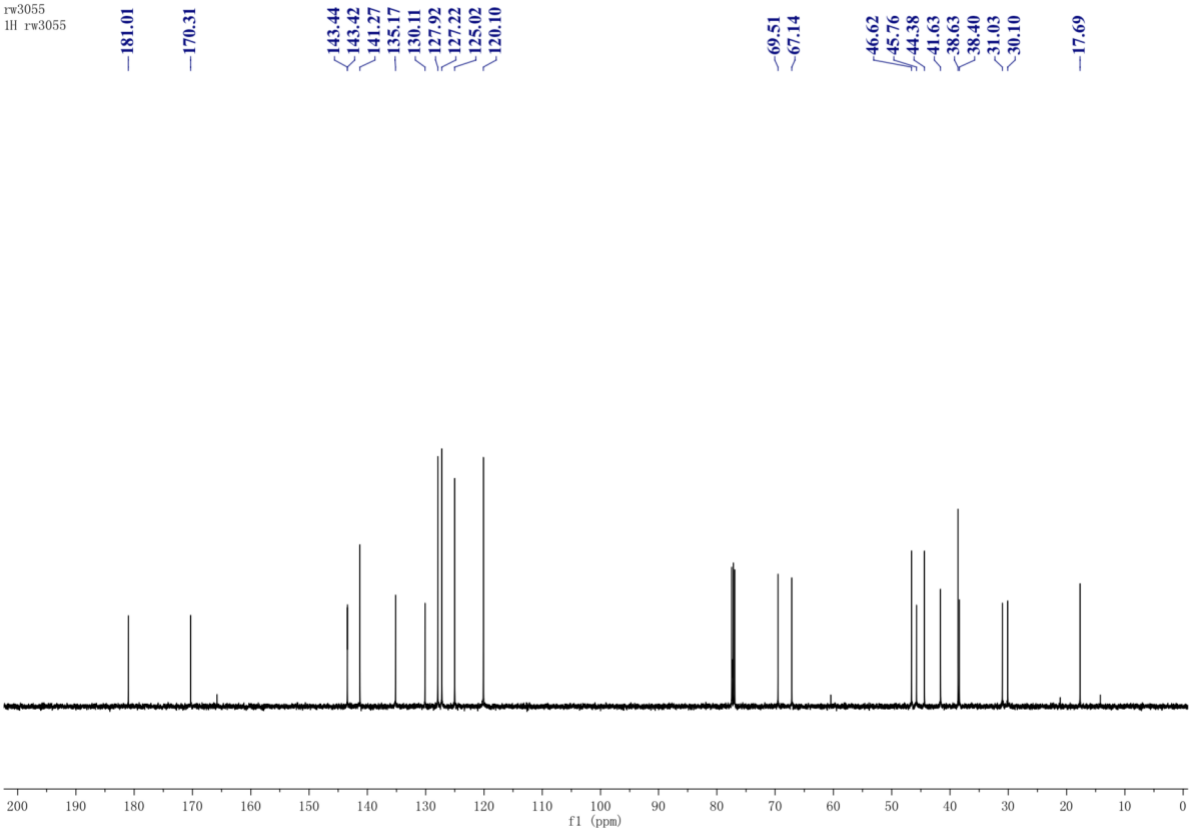

rw3057
1H rw3057

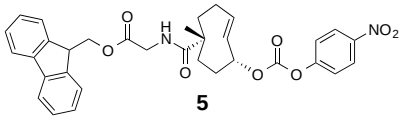

5

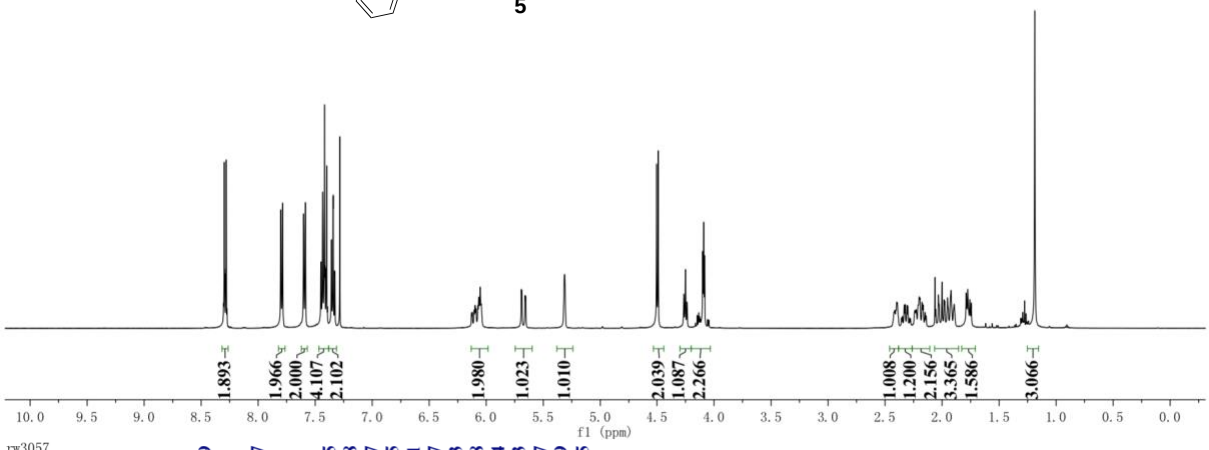

rw3057
13C rw3057

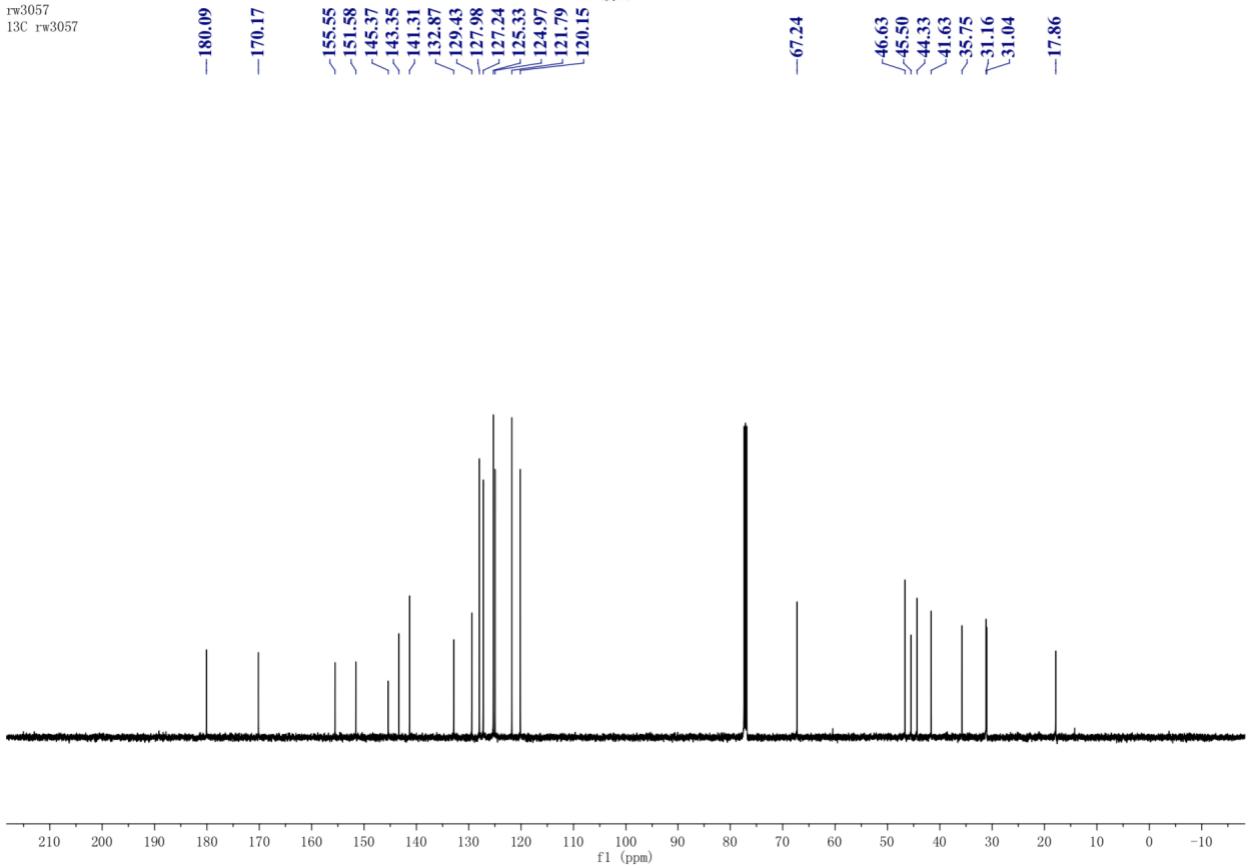

rw3066

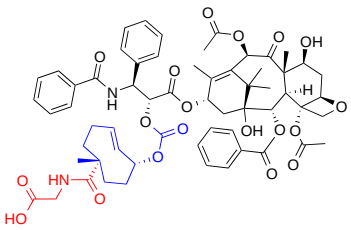

PTX-TCO-gly

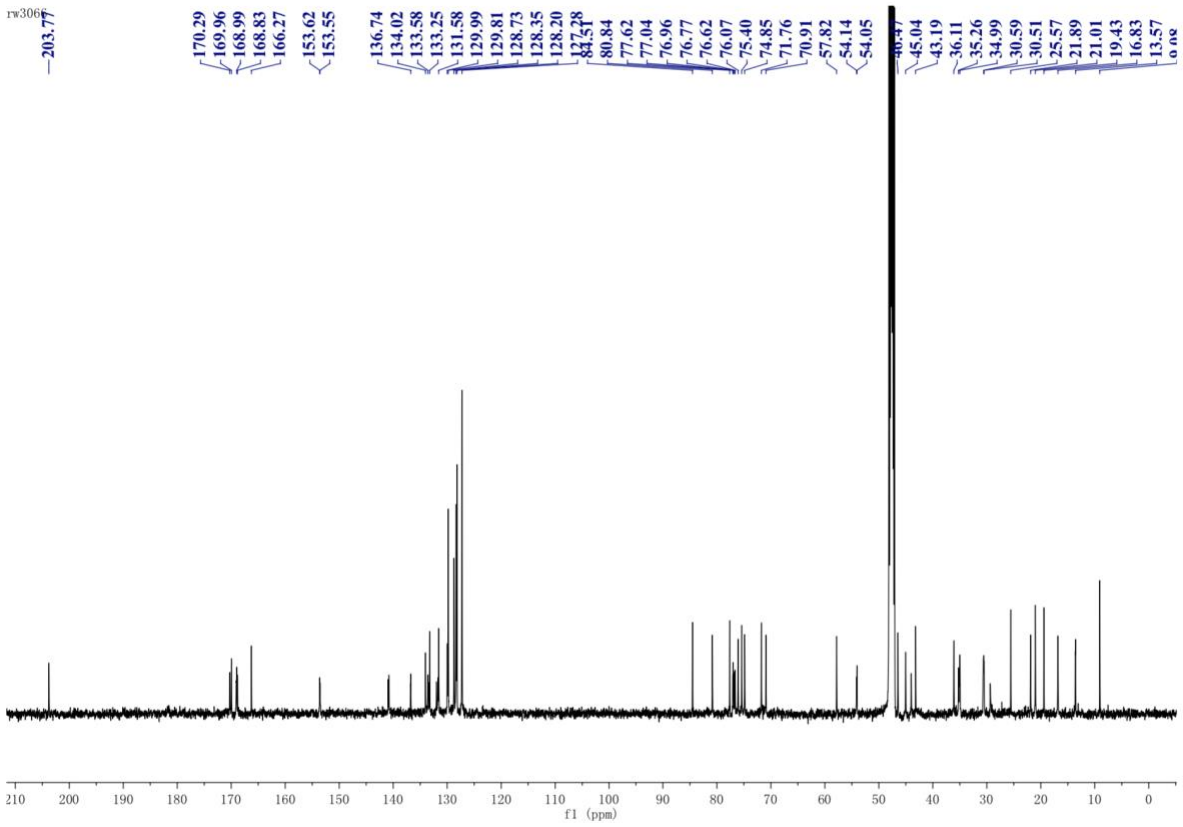

rw3159

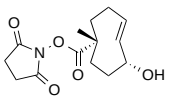

11

rw3159

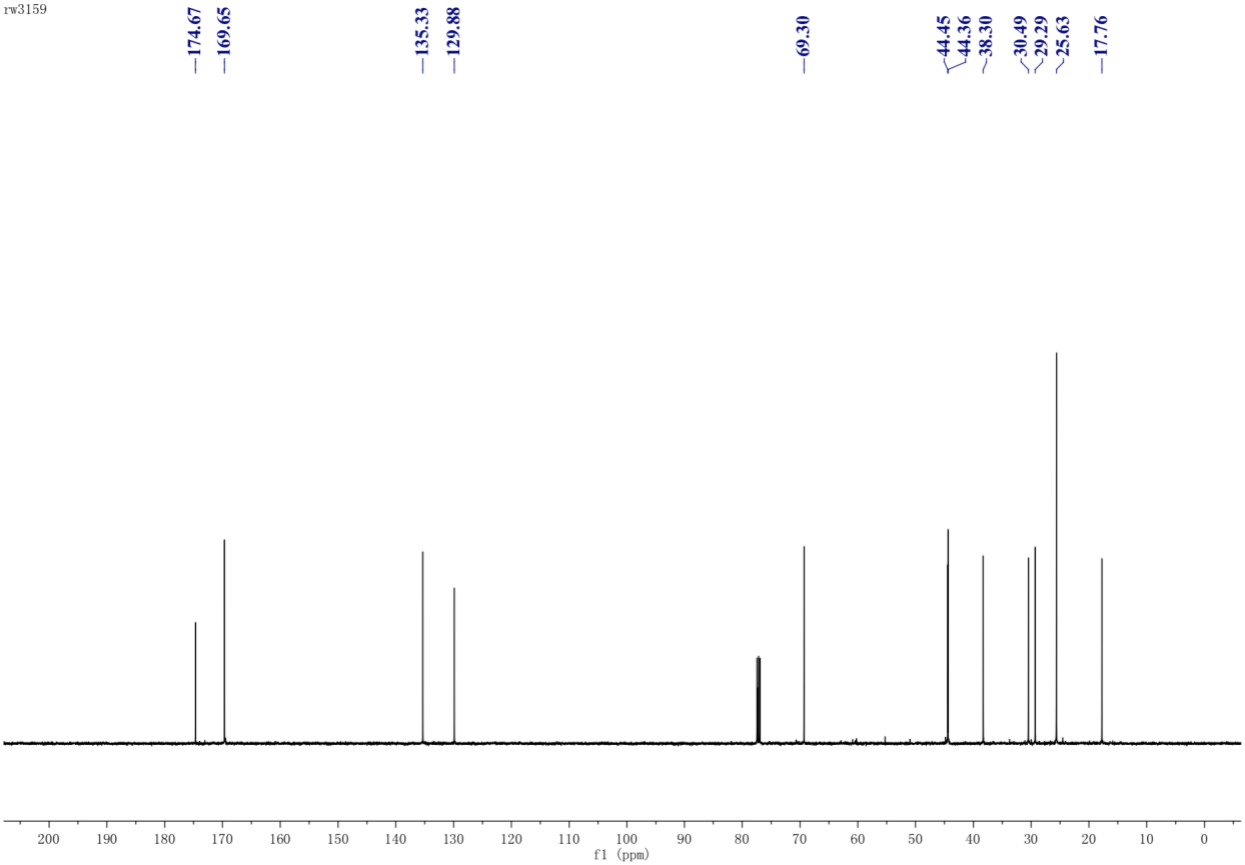

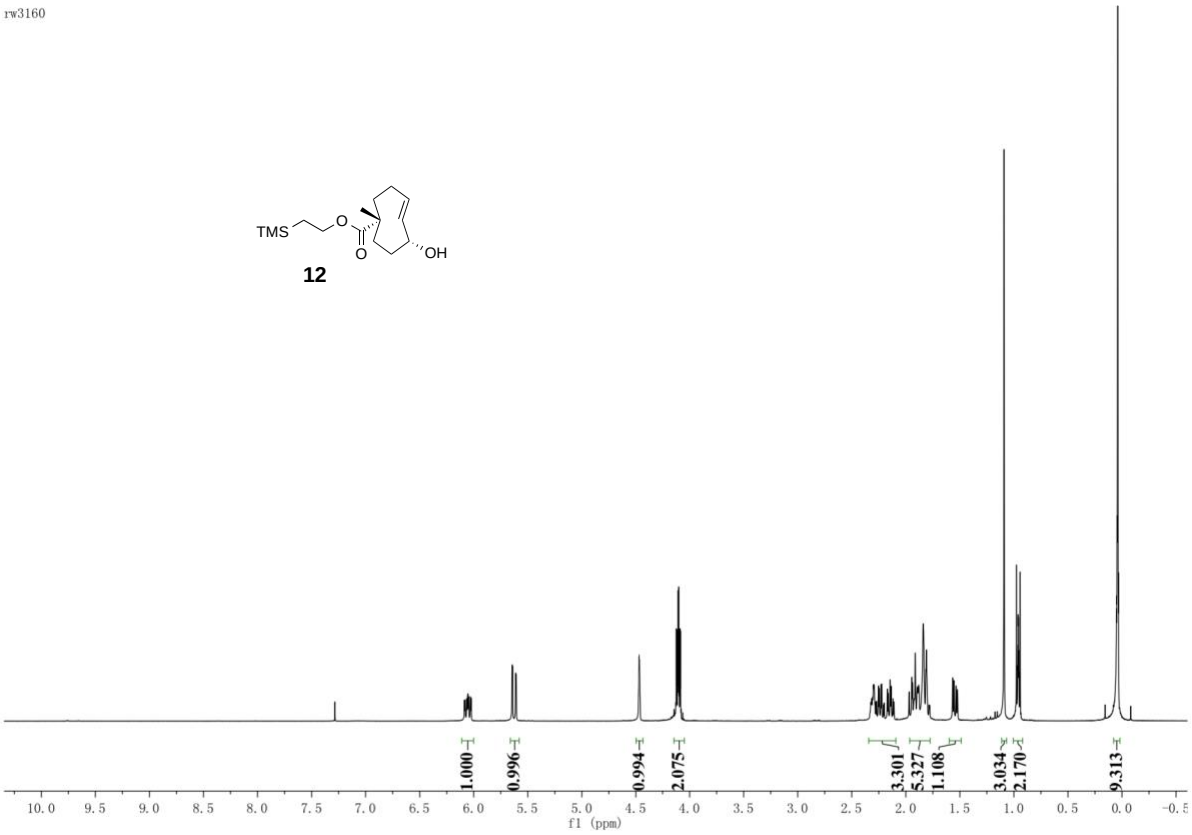
rw3160
TMS
O
O
O
OH
12
1.000
0.996
0.994
2.075
3.301
5.327
1.108
3.034
2.170
9.313
f1 (ppm)

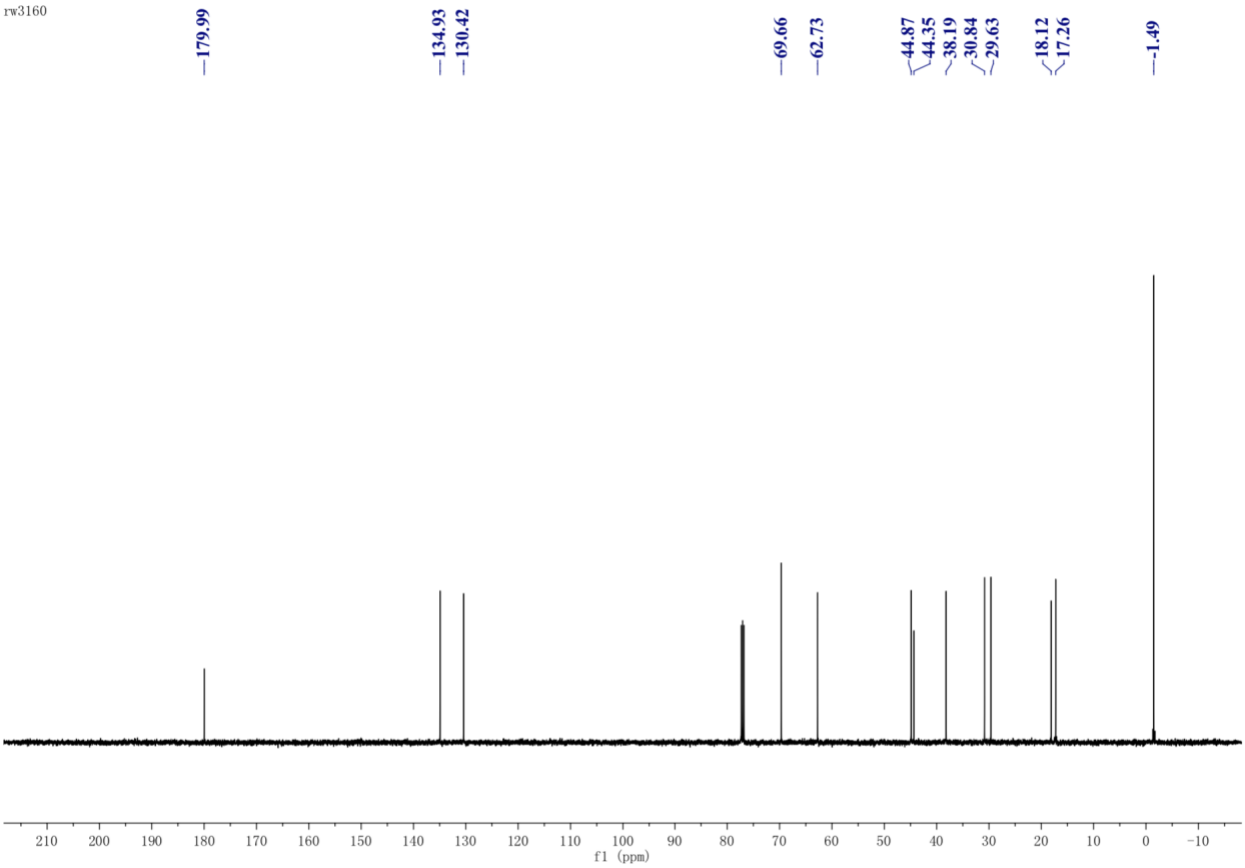
rw3160
179.99
134.93
130.42
69.66
62.73
44.87
44.35
38.19
30.84
29.63
18.12
17.26
-1.49
f1 (ppm)

rw2051
Proton rw2051

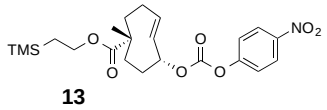

13

rw2051
13C rw2051

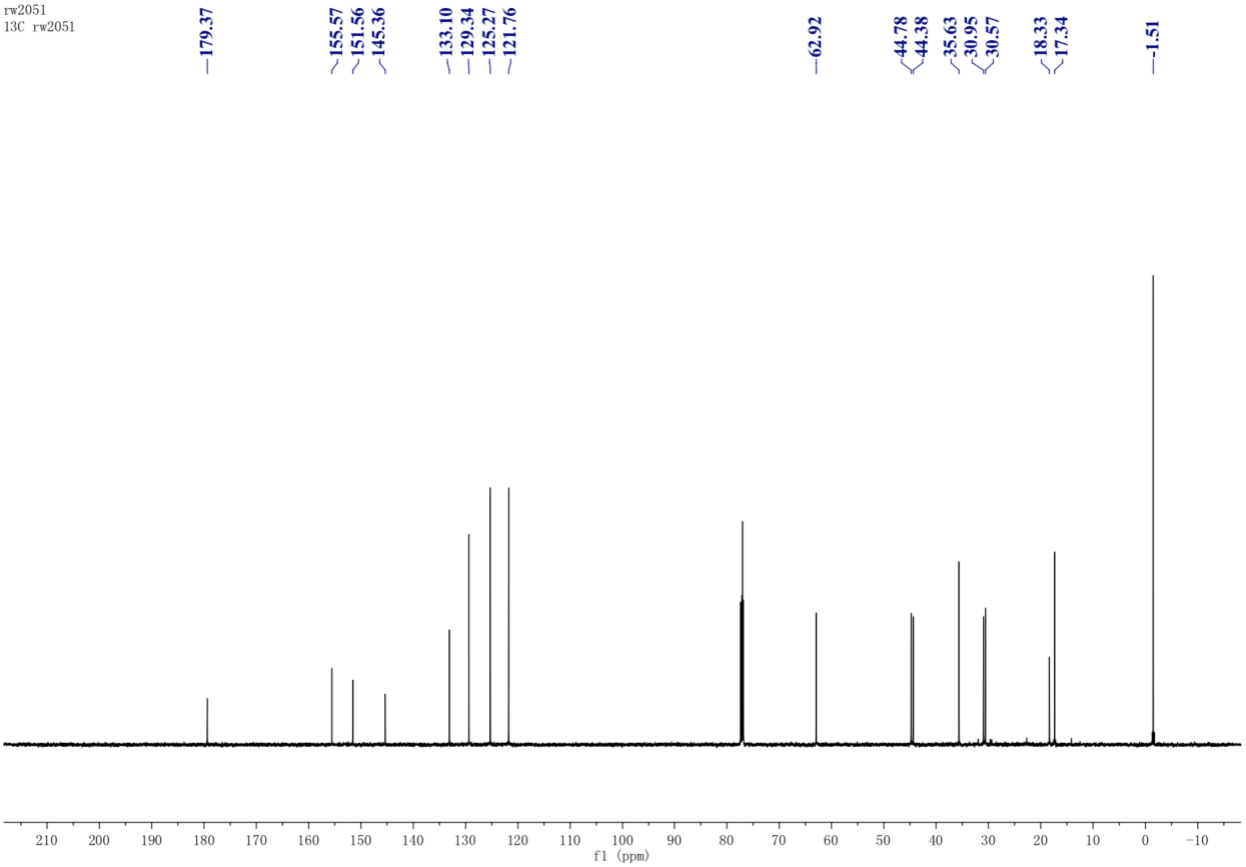

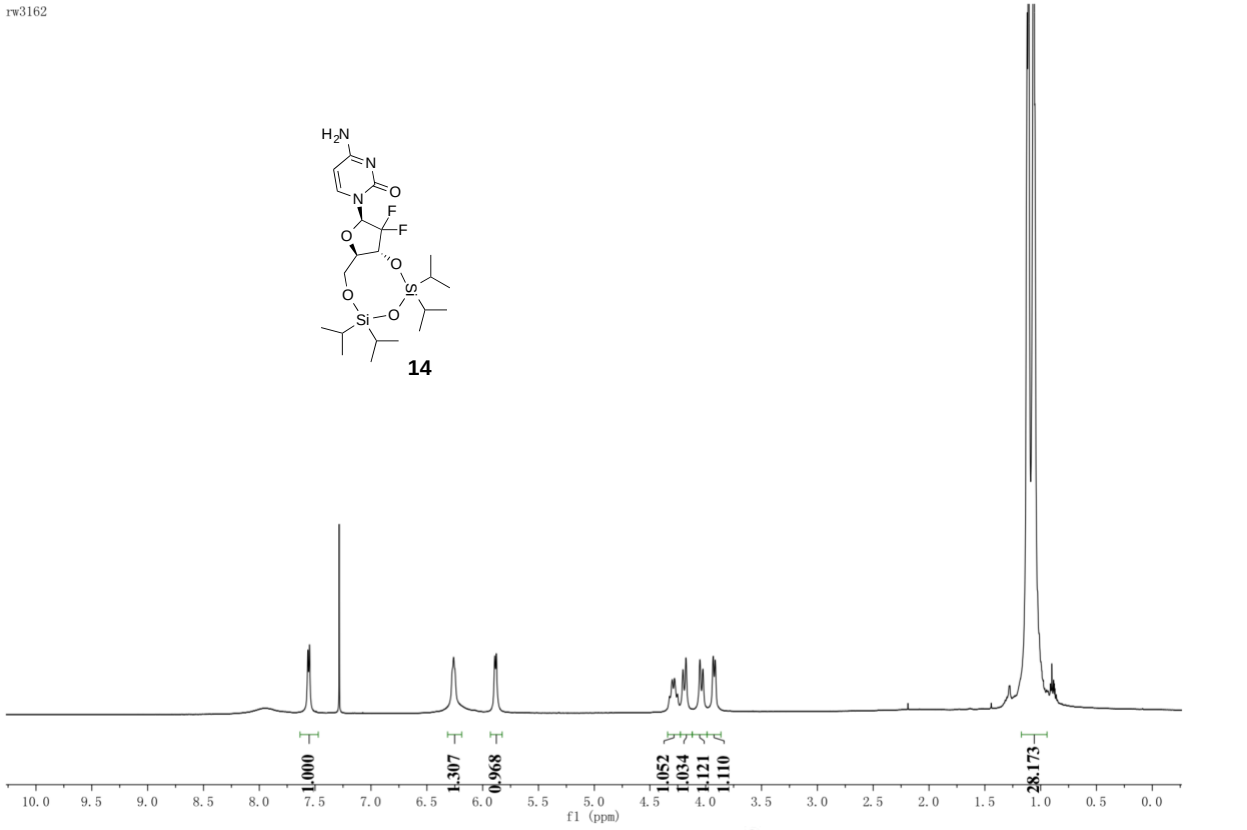
rw3162
1.000
1.307
0.968
1.052
1.034
1.121
1.110
28.173
f1 (ppm)

14

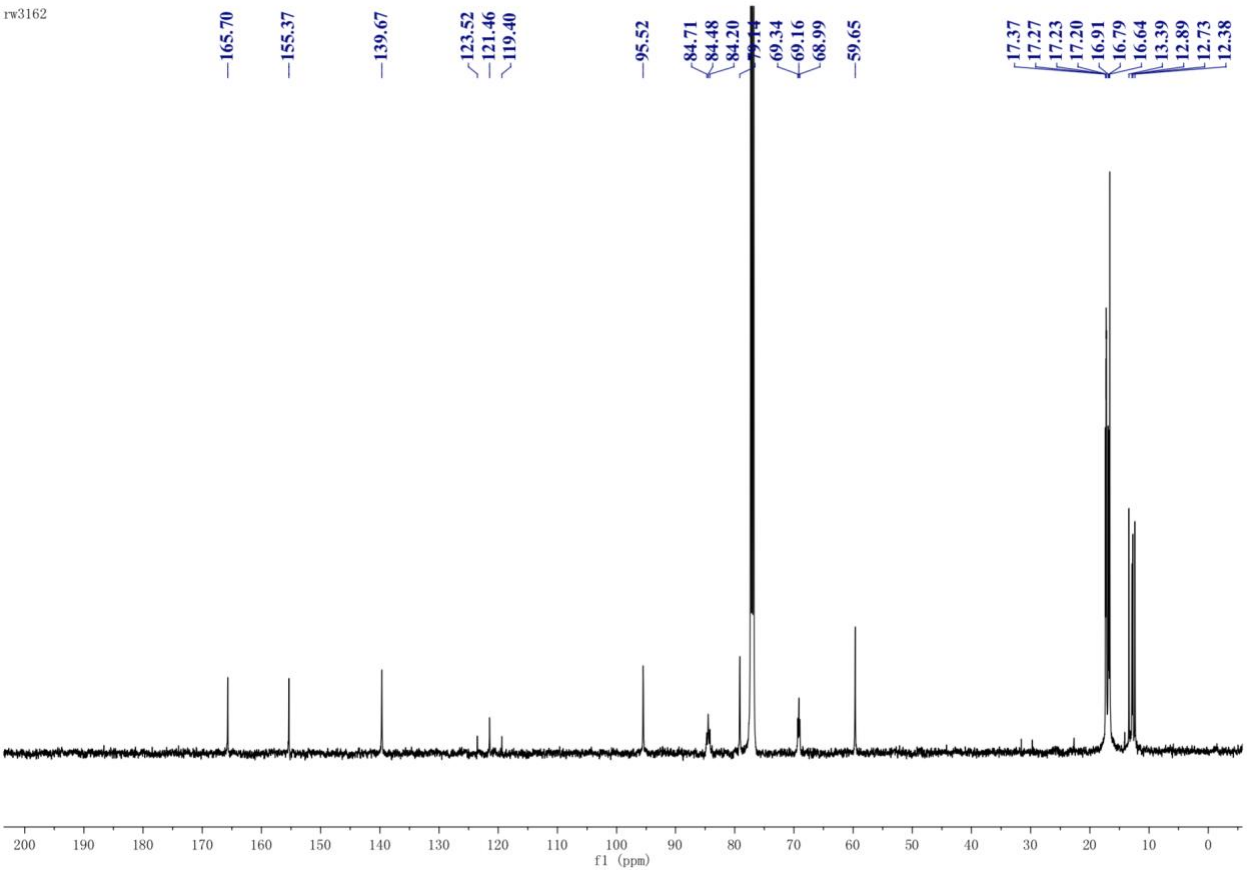
rw3162
165.70
155.37
139.67
123.52
121.46
119.40
95.52
84.71
84.48
84.20
79.14
69.34
69.16
68.99
59.65
17.37
17.27
17.23
17.20
16.91
16.79
16.64
13.39
12.89
12.73
12.38
f1 (ppm)

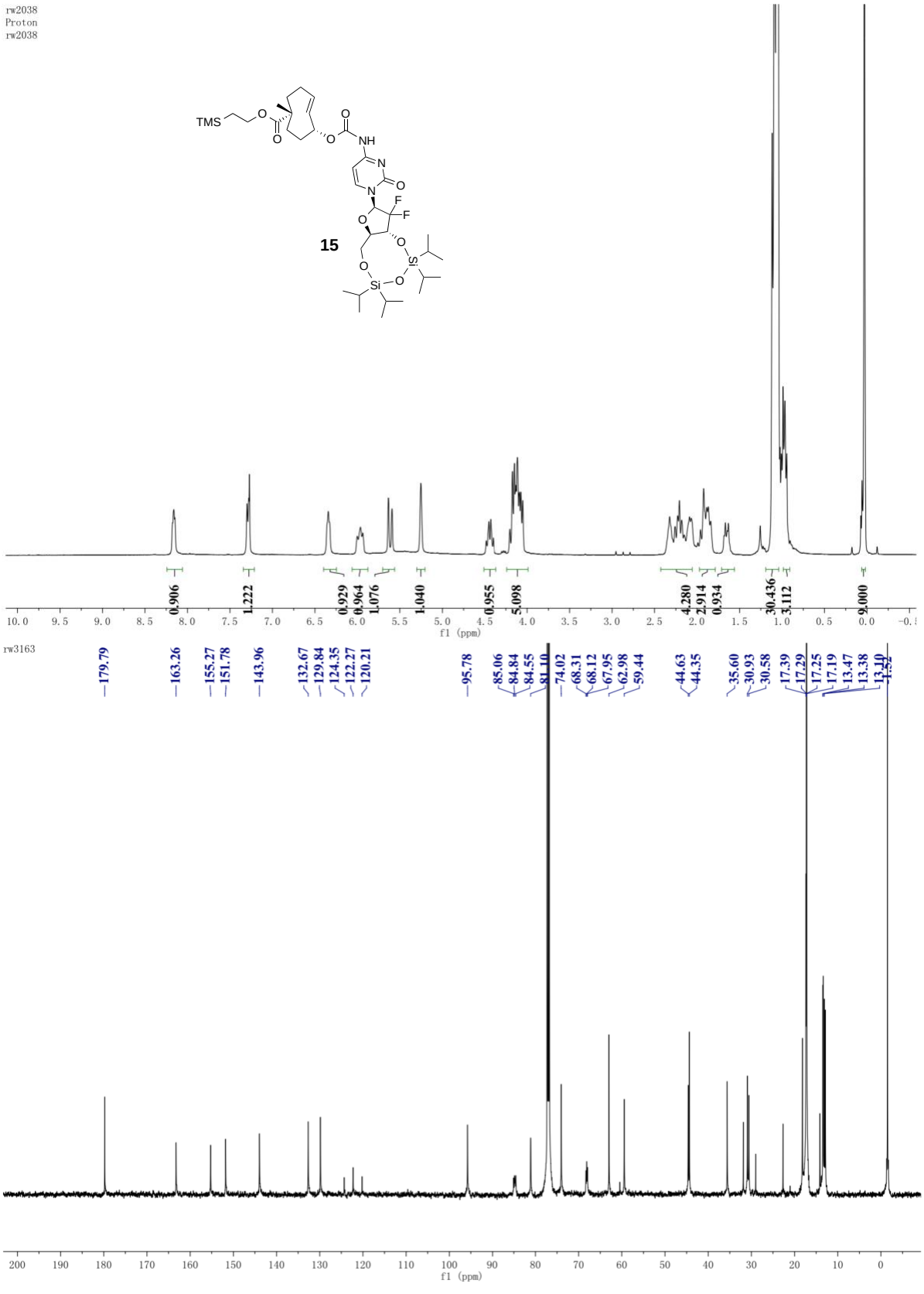
rw2038
Proton
rw2038
TMS
15
0.906
1.222
0.929
0.964
1.076
1.040
0.955
5.098
4.280
2.914
0.934
30.436
3.112
9.000
f1 (ppm)
rw3163
179.79
163.26
155.27
151.78
143.96
132.67
129.84
124.35
122.27
120.21
95.78
85.06
84.84
84.55
81.10
74.02
68.31
68.12
67.95
62.98
59.44
44.63
44.35
35.60
30.93
30.58
17.39
17.29
17.25
17.19
13.47
13.38
13.10
f1 (ppm)

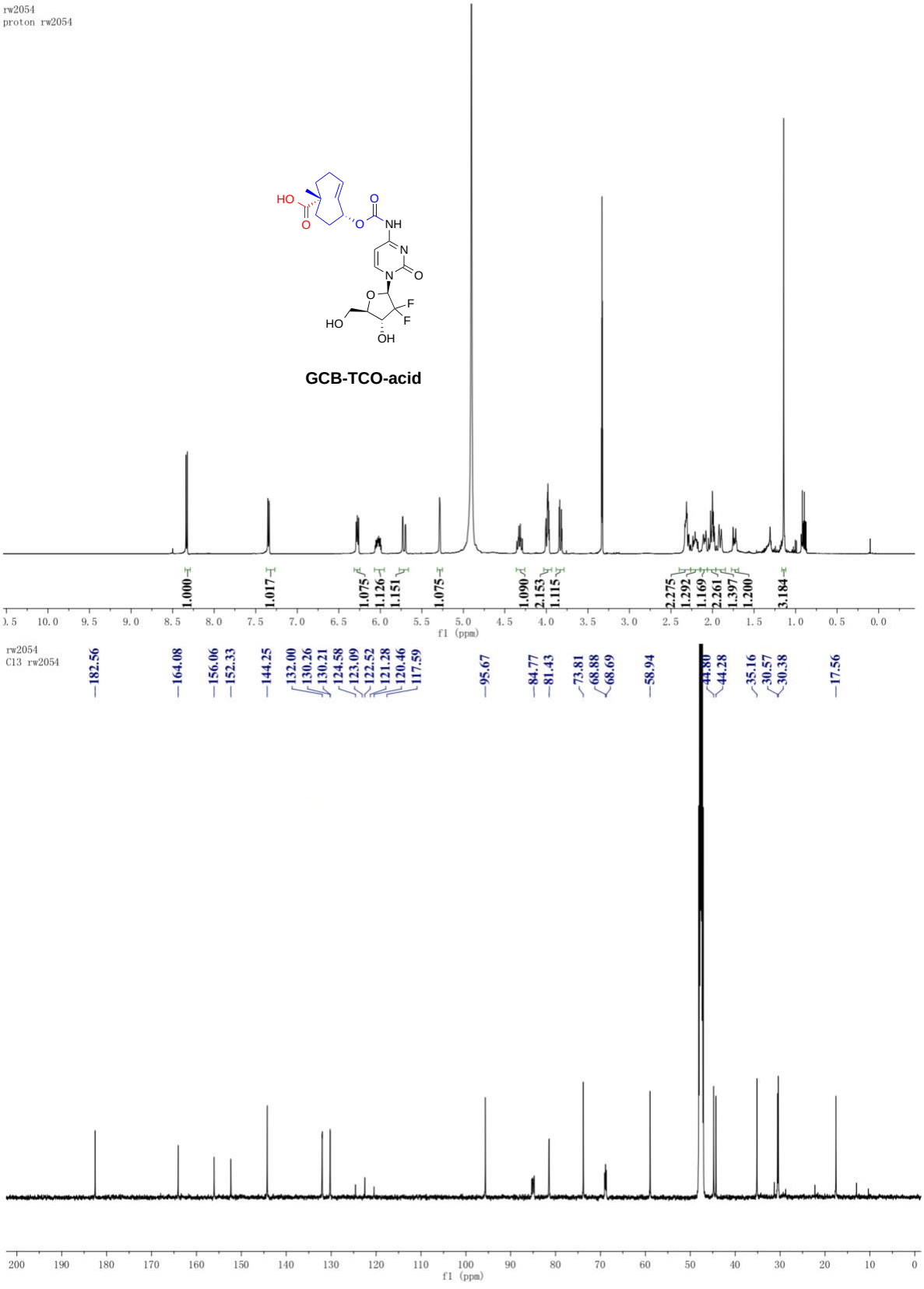
rw2054
proton rw2054
HO
O
O
O
NH
N
N
O
O
F
F
HO
OH
GCB-TCO-acid
1.000
1.017
1.075
1.126
1.151
1.075
1.090
2.153
1.115
2.275
1.292
1.169
2.261
1.397
1.200
3.184
f1 (ppm)
rw2054
C13 rw2054
182.56
164.08
156.06
152.33
144.25
132.00
130.26
130.21
124.58
123.09
122.52
121.28
120.46
117.59
95.67
84.77
81.43
73.81
68.88
68.69
58.94
44.80
44.28
35.16
30.57
30.38
17.56
f1 (ppm)